








TECH BRIEFS

NATIONAL AERONAUTICS AND SPACE ADMINISTRATION

-  **Technology Focus**
-  **Electronics/Computers**
-  **Software**
-  **Materials**
-  **Mechanics/Machinery**
-  **Manufacturing**
-  **Bio-Medical**
-  **Physical Sciences**
-  **Information Sciences**
-  **Books and Reports**

INTRODUCTION

Tech Briefs are short announcements of innovations originating from research and development activities of the National Aeronautics and Space Administration. They emphasize information considered likely to be transferable across industrial, regional, or disciplinary lines and are issued to encourage commercial application.

Additional Information on NASA Tech Briefs and TSPs

Additional information announced herein may be obtained from the NASA Technical Reports Server: <http://ntrs.nasa.gov>.

Please reference the control numbers appearing at the end of each Tech Brief. Information on NASA's Innovative Partnerships Program (IPP), its documents, and services is available on the World Wide Web at <http://www.ipp.nasa.gov>.

Innovative Partnerships Offices are located at NASA field centers to provide technology-transfer access to industrial users. Inquiries can be made by contacting NASA field centers listed below.

NASA Field Centers and Program Offices

Ames Research Center

Mary Walsh
(650) 604-1405
mary.w.walsh@nasa.gov

Dryden Flight Research Center

Ron Young
(661) 276-3741
ronald.m.young@nasa.gov

Glenn Research Center

Joe Shaw
(216) 977-7135
robert.j.shaw@nasa.gov

Goddard Space Flight Center

Nona Cheeks
(301) 286-5810
nona.k.cheeks@nasa.gov

Jet Propulsion Laboratory

Indrani Graczyk
(818) 354-2241
indrani.graczyk@jpl.nasa.gov

Johnson Space Center

John E. James
(281) 483-3809
john.e.james@nasa.gov

Kennedy Space Center

David R. Makufka
(321) 867-6227
david.r.makufka@nasa.gov

Langley Research Center

Michelle Ferebee
(757) 864-5617
michelle.t.ferebee@nasa.gov

Marshall Space Flight Center

Jim Dowdy
(256) 544-7604
jim.dowdy@nasa.gov

Stennis Space Center

Ramona Travis
(228) 688-3832
ramona.e.travis@ssc.nasa.gov

NASA Headquarters

Innovative Partnerships Office

Doug Comstock, Director
(202) 358-2221
doug.comstock@nasa.gov

Daniel Lockney,
Technology Transfer Lead
(202) 358-2037
daniel.p.lockney@nasa.gov

Small Business Innovation Research (SBIR) & Small Business Technology Transfer (STTR) Programs

Carl Ray, Program Executive
(202) 358-4652
carl.g.ray@nasa.gov



TECH BRIEFS

NATIONAL AERONAUTICS AND SPACE ADMINISTRATION



5 Technology Focus: Mechanical Components

- 5 Miniature, Variable-Speed Control Moment Gyroscope
- 5 NBL Pistol Grip Tool for Underwater Training of Astronauts
- 5 HEXPANDO Expanding Head for Fastener-Retention Hexagonal Wrench
- 6 Diagonal-Axes Stage for Pointing an Optical Communications Transceiver



7 Electronics/Computers

- 7 Improvements in Speed and Functionality of a 670-GHz Imaging Radar
- 7 IONAC-Lite
- 8 Large Ka-Band Slot Array for Digital Beam-Forming Applications
- 8 Development of a 150-GHz MMIC Module Prototype for Large-Scale CMB Radiation
- 9 Coupling Between Waveguide-Fed Slot Arrays
- 9 PCB-Based Break-Out Box
- 9 Multiple-Beam Detection of Fast Transient Radio Sources
- 10 Router Agent Technology for Policy-Based Network Management



11 Software

- 11 Remote Asynchronous Message Service Gateway
- 11 Automatic Tie Pointer for In-Situ Pointing Correction
- 11 Jitter Correction
- 12 MSLICE Sequencing
- 12 EOS MLS Level 2 Data Processing Software Version 3
- 12 DspaceOgre 3D Graphics Visualization Tool



13 Manufacturing & Prototyping

- 13 Metallization for Yb₁₄MnSb₁₁-Based Thermoelectric Materials
- 14 Solvent/Non-Solvent Sintering To Make Microsphere Scaffolds



15 Green Design

- 15 Enhanced Fuel-Optimal Trajectory-Generation Algorithm for Planetary Pinpoint Landing



17 Materials

- 17 Self-Cleaning Coatings and Materials for Decontaminating Field-Deployable Land and Water-Based Optical Systems

- 17 Separation of Single-Walled Carbon Nanotubes with DEP-FFF

- 18 Li Anode Technology for Improved Performance



19 Bio-Medical

- 19 Post-Fragmentation Whole Genome Amplification-Based Method
- 19 Microwave Tissue Soldering for Immediate Wound Closure
- 20 Principles, Techniques, and Applications of Tissue Microfluidics
- 21 Robotic Scaffolds for Tissue Engineering and Organ Growth
- 21 Stress-Driven Selection of Novel Phenotypes



23 Physical Sciences

- 23 Method for Accurately Calibrating a Spectrometer Using Broadband Light
- 23 Catalytic Microtube Rocket Igniter
- 24 Stage Cylindrical Immersive Display
- 25 Vacuum Camera Cooler
- 25 Atomic Oxygen Fluence Monitor



27 Information Sciences

- 27 Thermal Management Tools for Propulsion System Trade Studies and Analysis
- 27 Introduction to Physical Intelligence
- 27 Technique for Solving Electrically Small to Large Structures for Broadband Applications
- 28 Accelerated Adaptive MGS Phase Retrieval
- 28 Large Eddy Simulation Study for Fluid Disintegration and Mixing
- 29 Tropospheric Correction for InSAR Using Interpolated ECMWF Data and GPS Zenith Total Delay
- 30 Technique for Calculating Solution Derivatives With Respect to Geometry Parameters in a CFD Code
- 30 Acute Radiation Risk and BRYNTRN Organ Dose Projection Graphical User Interface
- 31 Probabilistic Path Planning of Montgolfier Balloons in Strong, Uncertain Wind Fields



33 Books & Reports

- 33 Flight Simulation of ARES in the Mars Environment
- 33 Low-Outgassing Photogrammetry Targets for Use in Outer Space
- 33 Planning the FUSE Mission Using the SOVA Algorithm
- 33 Monitoring Spacecraft Telemetry Via Optical or RF Link
- 34 Robust Thermal Control of Propulsion Lines for Space Missions

This document was prepared under the sponsorship of the National Aeronautics and Space Administration. Neither the United States Government nor any person acting on behalf of the United States Government assumes any liability resulting from the use of the information contained in this document, or warrants that such use will be free from privately owned rights.



⚙️ **Miniature, Variable-Speed Control Moment Gyroscope**

Goddard Space Flight Center, Greenbelt, Maryland

The Miniature Variable-Speed Control Moment Gyroscope (MVS-CMG) was designed for small satellites (mass from less than 1 kg up to 500 kg). Currently available CMGs are too large and heavy, and available miniature CMGs do not provide sufficient control authority for use on practical satellites. This primarily results from the need to greatly increase the speed of rotation of the flywheel in order to reduce the flywheel size and mass. This goal was achieved by making use of a proprietary, space-qualified, high-speed (100,000 rpm) motor technology to spin the flywheel at a speed ten times faster than other known miniature CMGs under development.

NASA is supporting innovations in propulsion, power, and guidance and navigation systems for low-cost small spacecraft. One of the key enabling technologies is attitude control mechanisms. CMGs are particularly attractive for spacecraft attitude control since they can achieve higher torques with lower mass and power than reaction wheels, and they provide continuous torque capability that enables precision pointing (in contrast to on-off thruster control).

The aim of this work was to develop a miniature, variable-speed CMG that is sized for use on small satellites. To achieve improved agility, these space-

craft must be able to slew at high rate, which requires attitude control actuators that can apply torques on the order of 5 N·m. The MVS-CMG is specifically designed to achieve a high-torque output with a minimum flywheel and system mass. The flywheel can be run over a wide range of speeds, which is important to help reduce/eliminate potential gimbal lock, and can be used to optimize the operational envelope of the CMG.

This work was done by Steve Bilski, Robert Kline-Schoder, and Paul Sorensen of Creare Inc. for Goddard Space Flight Center. Further information is contained in a TSP (see page 1). GSC-15887-1

⚙️ **NBL Pistol Grip Tool for Underwater Training of Astronauts**

Goddard Space Flight Center, Greenbelt, Maryland

A document discusses a lightweight, functional mockup of the Pistol Grip Tool for use during underwater astronaut training. Previous training tools have caused shoulder injuries. This new version is more than 50 percent lighter [in water, weight is 2.4 lb (≈1.1 kg)], and can operate for a six-hour training session after 30 minutes of prep for submersion.

Innovations in the design include the use of lightweight materials (aluminum and Delrin®), creating a thinner housing, and the optimization of internal space with the removal of as much excess material as possible. This reduces tool weight and maximizes buoyancy. Another innovation for this tool is the application of a vacuum that seats the O-

rings in place and has shown to be reliable in allowing underwater usage for up to six hours.

This work was done by Michael Liszka, Matthew Ashmore, Mark Behnke, Walter Smith, and Tod Waterman of ATK Spacecraft, Systems and Services for Goddard Space Flight Center. Further information is contained in a TSP (see page 1). GSC-16060-1

⚙️ **HEXPANDO Expanding Head for Fastener-Retention Hexagonal Wrench**

Goddard Space Flight Center, Greenbelt, Maryland

The HEXPANDO is an expanding-head hexagonal wrench designed to retain fasteners and keep them from being dislodged from the tool. The tool is intended to remove or install socket-head cap screws (SHCSs) in remote, hard-to-reach locations or in circumstances when a dropped fastener could cause damage to delicate or sensitive hardware. It is not intended for application of torque.

This tool is made of two assembled portions. The first portion of the tool comprises tubing, or a hollow shaft, at a length that gives the user adequate reach to the intended location. At one end of the tubing is the expanding hexagonal headfitting with six radial slits cut into it (one at each of the points of the hexagonal shape), and a small hole drilled axially through the center and the end opposite the hex is

internally and externally threaded. This fitting is threaded into the shaft (via external threads) and staked or bonded so that it will not loosen. At the other end of the tubing is a knurled collar with a through hole into which the tubing is threaded. This knob is secured in place by a stop nut.

The second assembled portion of the tool comprises a length of all thread or solid rod that is slightly longer than the

steel tubing. One end has a slightly larger knurled collar affixed while the other end is tapered/pointed and threaded. When the two portions are assembled, the all thread/rod portion feeds through the tubing and is threaded into the expanding hex head fitting. The tapered point allows it to be driven into the through hole of the hex fitting. While holding the smaller collar on the shaft, the user turns the larger

collar, and as the threads feed into the fitting, the hex head expands and grips the SHCS, thus providing a safe way to install and remove fasteners. The clamping force retaining the SHCS varies depending on how far the tapered end is inserted into the tool head.

Initial tests of the prototype tool, designed for a 5 mm or # 10SHCS have resulted in up to 8 lb (≈ 35.6 N) of pull force to dislodge the SHCS from the

tool. The tool is designed with a lead-in angle from the diameter of the tubing to a diameter the same as the fastener head, to prevent the fastener head from catching on any obstructions encountered that could dislodge the fastener during retrieval.

This work was done by John Bishop of QinetiQ for Goddard Space Flight Center. Further information is contained in a TSP (see page 1). GSC-16109-1

⚙️ Diagonal-Axes Stage for Pointing an Optical Communications Transceiver

Potential applications include steering aircraft-mounted cameras for ground imaging.

NASA's Jet Propulsion Laboratory, Pasadena, California

Traditional azimuth-elevation (“az-el”) stages are used to point a variety of devices ranging from large optical telescopes to tank guns. Such a stage typically has an “elevation” stage having a horizontal axis mounted on an “azimuth” stage with a vertical axis. Both stages are often motorized.

Optical communications transceivers often require two-axis motorized control, as when the communications link is between a ground station and an aircraft or

satellite. In such applications, the traditional azimuth-elevation stage has two important drawbacks: a “gimbal lock” exclusion zone at zenith and susceptibility to pointing errors caused by backlash. Az-el stages in which the azimuth stage cannot rotate a full 360° have the additional drawback of an azimuth exclusion zone.

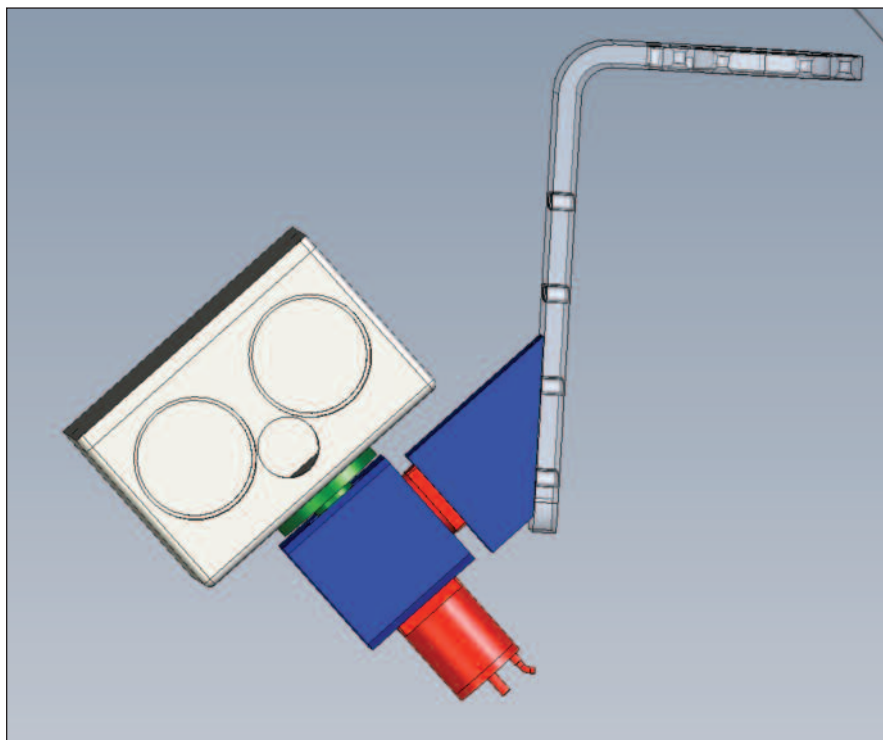
The diagonal-axes stage described here mitigates or eliminates all of these problems. Instead of one vertical axis and one

horizontal axis, a diagonal-axes stage has two horizontal axes, both oriented at 45° to the trajectory of the target. For example, a ground station located on the equator tracking a satellite with an equatorial orbit would have one axis parallel to northeast and southwest, and the other axis parallel to northwest and southeast.

The diagonal-axes stage is considerably less vulnerable to backlash. If it is correctly oriented, its axes rotate in only one direction during an overhead pass by a satellite. As a result, the effects of backlash may be inherently eliminated. If the gravity-induced torque on either axis changes during the pass, then backlash may become important during the part of the pass where the gravity torque, instead of opposing the motion of the stage, pushes the stage in the direction of motion. This can result in the loss of gear-to-gear contact in one or more stages of the gear reduction mechanism. In this case, a preload spring used to eliminate backlash need only be sufficiently strong to overcome the gravity torque, i.e. it need not overcome friction in the gear train.

The diagonal-axes stage is not backlash-free for arbitrary target trajectories such as an aircraft might execute. If properly oriented for any particular satellite, however, it is backlash-free for all passes of that satellite, which will trace out parallel paths on the sky, and for all passes of any other satellite that are perpendicular to the first. It will also be backlash-free for some fraction of other satellite trajectories.

This work was done by Martin W. Regehr and Vachik Garkanian of Caltech for NASA's Jet Propulsion Laboratory. Further information is contained in a TSP (see page 1). NPO-47427



A design based on the Diagonal-Axes Stage principle. Motors are shown in red, wedge and intermotor block are shown in blue, and the payload hub is green. The box at left with three circular apertures is an example of an optical payload; the L-bracket at left is a mounting bracket supporting the stage. Direction of travel is right-to-left.



Improvements in Speed and Functionality of a 670-GHz Imaging Radar

Image acquisition time has been reduced, enabling clearer images of contraband objects hidden underneath clothing.

NASA's Jet Propulsion Laboratory, Pasadena, California

Significant improvements have been made in the instrument originally described in a prior *NASA Tech Briefs* article: "Improved Speed and Functionality of a 580-GHz Imaging Radar" (NPO-45156), Vol. 34, No. 7 (July 2010), p. 51. First, the wideband YIG oscillator has been replaced with a JPL-designed and built phase-locked, low-noise chirp source. Second, further refinements to the data acquisition and signal processing software have been performed by moving critical code sections to C code, and compiling those sections to Windows DLLs, which are then invoked from the main LabVIEW executive.

This system is an active, single-pixel scanned imager operating at 670 GHz. The actual chirp signals for the RF and LO chains were generated by a pair of MITEQ 2.5–3.3 GHz chirp sources. Agilent benchtop synthesizers operating at fixed frequencies around 13 GHz were then used to up-convert the chirp sources to 15.5–16.3 GHz. The resulting signals were then multiplied 36 times by

a combination of off-the-shelf millimeter-wave components, and JPL-built 200-GHz doublers and 300- and 600-GHz triplers. The power required to drive the submillimeter-wave multipliers was provided by JPL-built W-band amplifiers. The receive and transmit signal paths were combined using a thin, high-resistivity silicon wafer as a beam splitter.

While the results at present are encouraging, the system still lacks sufficient speed to be usable for practical applications in a contraband detection. Ideally, an image acquisition speed of ten seconds, or a factor of 30 improvement, is desired. However, the system improvements to date have resulted in a factor of five increase in signal acquisition speed, as well as enhanced signal-processing algorithms, permitting clearer imaging of contraband objects hidden underneath clothing. In particular, advances in three distinct areas have enabled these performance enhancements: base source phase noise reduction, chirp rate, and signal pro-

cessing. Additionally, a second pixel was added, automatically reducing the imaging time by a factor of two. Although adding a second pixel to the system doubles the amount of submillimeter components required, some savings in microwave hardware can be realized by using a common low-noise source.

This work was done by Robert J. Dengler, Ken B. Cooper, Imran Mehdi, Peter H. Siegel, Jan A. Tarsala, and Tomas E. Bryllert of Caltech for NASA's Jet Propulsion Laboratory. For more information, contact iaoffice@jpl.nasa.gov.

In accordance with Public Law 96-517, the contractor has elected to retain title to this invention. Inquiries concerning rights for its commercial use should be addressed to:

*Innovative Technology Assets Management
JPL*

Mail Stop 202-233

4800 Oak Grove Drive

Pasadena, CA 91109-8099

E-mail: iaoffice@jpl.nasa.gov

Refer to NPO-47180, volume and number of this NASA Tech Briefs issue, and the page number.

IONAC-Lite

A combination of energy and performance optimization is attained for high-speed Delay Tolerant Networking.

NASA's Jet Propulsion Laboratory, Pasadena, California

The Interplanetary Overlay Networking Protocol Accelerator (IONAC) described previously in "The Interplanetary Overlay Networking Protocol Accelerator" (NPO-45584), *NASA Tech Briefs*, Vol. 32, No. 10, (October 2008) p. 106 (<http://www.techbriefs.com/component/content/article/3317>) provides functions that implement the Delay Tolerant Networking (DTN) bundle protocol. New missions that require high-speed downlink-only use of DTN can now be accommodated by the unidirectional IONAC-Lite to support high

data rate downlink mission applications. Due to constrained energy resources, a conventional software implementation of the DTN protocol can provide only limited throughput for any given reasonable energy consumption rate. The IONAC-Lite DTN Protocol Accelerator is able to reduce this energy consumption by an order of magnitude and increase the throughput capability by two orders of magnitude. In addition, a conventional DTN implementation requires a bundle database with a considerable storage re-

quirement. In very high downlink data-rate missions such as near-Earth radar science missions, the storage space utilization needs to be maximized for science data and minimized for communications protocol-related storage needs.

The IONAC-Lite DTN Protocol Accelerator is implemented in a reconfigurable hardware device to accomplish exactly what's needed for high-throughput DTN downlink-only scenarios.

The following are salient features of the IONAC-Lite implementation:

- An implementation of the Bundle Pro-

tol for an environment that requires a very high rate bundle egress data rate. The C&DH (command and data handling) subsystem is also expected to be very constrained so the interaction with the C&DH processor and the temporary storage are minimized.

- Fully pipelined design so that bundle processing database is not required.
- Implements a lookup table-based approach to eliminate multi-pass process-

ing requirement imposed by the Bundle Protocol header's length field structure and the SDNV (self-delimiting numeric value) data field formatting.

- 8-bit parallel datapath to support high data-rate missions.
- Reduced resource utilization implementation for missions that do not require custody transfer features. There was no known implementation of the DTN protocol in a field programmable

gate array (FPGA) device prior to the current implementation.

The combination of energy and performance optimization that embodies this design makes the work novel.

This work was done by Jordan L. Torgerson, Loren P. Clare, and Jackson Pang of Caltech for NASA's Jet Propulsion Laboratory. For more information, contact the JPL Innovative Technology Assets Management Office, 1-818-393-3421, and reference NPO-47344.

Large Ka-Band Slot Array for Digital Beam-Forming Applications

NASA's Jet Propulsion Laboratory, Pasadena, California

This work describes the development of a large Ka Band Slot Array for the Glacier and Land Ice Surface Topography Interferometer (GLISTIN), a proposed spaceborne interferometric synthetic aperture radar for topographic mapping of ice sheets and glaciers. GLISTIN will collect ice topography measurement data over a wide swath with sub-seasonal repeat intervals using a Ka-band digitally beam-formed antenna.

For technology demonstration purpose a receive array of size 1x1 m, consisting of 160x160 radiating elements, was developed. The array is divided into 16 sticks, each stick consisting of 160x10 radiating elements, whose outputs are combined to produce 16 digital beams. A transmit array stick was also developed. The antenna arrays were designed using Elliott's design equations with the

use of an infinite-array mutual-coupling model. A Floquet wave model was used to account for external coupling between radiating slots. Because of the use of uniform amplitude and phase distribution, the infinite array model yielded identical values for all radiating elements but for alternating offsets, and identical coupling elements but for alternating positive and negative tilts.

Waveguide-fed slot arrays are finding many applications in radar, remote sensing, and communications applications because of their desirable properties such as low mass, low volume, and ease of design, manufacture, and deployability. Although waveguide-fed slot arrays have been designed, built, and tested in the past, this work represents several advances to the state of the art. The use of the infinite array model for the radiating

slots yielded a simple design process for radiating and coupling slots. Method of moments solution to the integral equations for alternating offset radiating slots in an infinite array environment was developed and validated using the commercial finite element code HFSS. For the analysis purpose, a method of moments code was developed for an infinite array of subarrays.

Overall the 1x1 m array was found to be successful in meeting the objectives of the GLISTIN demonstration antenna, especially with respect to the 0.042°, 1/10th of the beamwidth of each stick, relative beam alignment between sticks.

This work was done by Sembiam Rengaranjan, Mark S. Zawadzki, and Richard E. Hodges of Caltech for NASA's Jet Propulsion Laboratory. For more information, contact iaoffice@jpl.nasa.gov. NPO-47416

Development of a 150-GHz MMIC Module Prototype for Large-Scale CMB Radiation

NASA's Jet Propulsion Laboratory, Pasadena, California

HEMT-based receiver arrays with excellent noise and scalability are already starting to be manufactured at 100 GHz, but the advances in technology should make it possible to develop receiver modules with even greater operation frequency up to 200 GHz. A prototype heterodyne amplifier module has been developed for operation from 140 to 170 GHz using monolithic millimeter-wave integrated circuit (MMIC) low-noise InP high electron mobility transistor (HEMT) amplifiers.

The compact, scalable module is centered on the 150-GHz atmospheric win-

dow using components known to operate well at these frequencies. Arrays equipped with hundreds of these modules can be optimized for many different astrophysical measurement techniques, including spectroscopy and interferometry.

This module is a heterodyne receiver module that is extremely compact, and makes use of 35-nm InP HEMT technology, and which has been shown to have excellent noise temperatures when cooled cryogenically to 30 K. This reduction in system noise over prior art has been demonstrated in commercial mixers (uncooled) at frequencies of

160–180 GHz. The module is expected to achieve a system noise temperature of 60 K when cooled.

An MMIC amplifier module has been designed to demonstrate the feasibility of expanding heterodyne amplifier technology to the 140 to 170-GHz frequency range for astronomical observations. The miniaturization of many standard components and the refinement of RF interconnect technology have cleared the way to mass-production of heterodyne amplifier receivers, making it a feasible technology for many large-population arrays.

This work furthers the recent research efforts in compact coherent receiver modules, including the development of the Q/U Imaging Experiment (QUIET) modules centered at 40 and 90 GHz, and the pro-

duction of heterodyne module prototypes at 90 GHz.

This work was done by Pekka P. Kangaslahti, Lorene A. Samoska, Todd C. Gaier, and Mary M. Soria of Caltech; Patricia E. Voll, Sarah E. Church, Judy M. Lau, and

Matthew M. Sieth of Stanford University; and Daniel Van Winkle and Sami Tantawi of SLAC National Accelerator Laboratory for NASA's Jet Propulsion Laboratory. Further information is contained in a TSP (see page 1). NPO-47664

Coupling Between Waveguide-Fed Slot Arrays

NASA's Jet Propulsion Laboratory, Pasadena, California

Coupling between two waveguide-fed planar slot arrays has been investigated using full-wave analysis. The analysis employs the method-of-moments solution to the pertinent coupled integral equations for the aperture electric field of all slots. In order to compute coupling between two arrays, the input port of the first array is excited with a TE₁₀ mode wave while the second one is match-terminated. After solving the moment method matrix equations, the aperture fields of all slots are obtained and

thereby the TE₁₀ mode wave received at the input port of the second array is determined. Coupling between two arrays is the ratio of the wave amplitude arriving in the second array port to the incident wave amplitude at the first array port. The coupling mechanism has been studied as a function of spacing between arrays in different directions, e.g. the electric field plane, the magnetic field plane, and the diagonal plane. Computed coupling values are presented for different array geometries.

This work is novel since it provides a good understanding of coupling between waveguide-fed slot arrays as a function of spacing and orientation for different aperture distributions and array architectures. This serves as a useful tool for antenna design engineers and system engineers.

This work was done by Sembiam Rengaranjan of Caltech for NASA's Jet Propulsion Laboratory. For more information, contact iaoffice@jpl.nasa.gov. NPO-47446

PCB-Based Break-Out Box

NASA's Jet Propulsion Laboratory, Pasadena, California

Break-out boxes (BOBs) are necessary for all electrical integration/cable checkouts and troubleshooting. Because the price of a BOB is high, and no work can be done without one, often the procedure stops, simply waiting for a BOB. A less expensive BOB would take less time in the integration, testing, and troubleshooting process.

The PCB-based BOB works and looks the same as a standard JPL BOB, called "Gold Boxes." The only differences between the old BOB and the new PCB-based BOB is that the new one has 80 percent of its circuitry in a printed circuit

board. This process reduces the time for fabrication, thus making the BOBs less expensive. Moreover, because of its unique design, the new BOBs can be easily assembled and fixed. About 80 percent of the new PCB-based BOB is in a \$22 (at the time of this reporting) custom-designed, yet commercially available PCB.

This device has been used successfully to verify that BOB cables were properly made. Also, upon completion, the BOB was beeped out via a multimeter to ensure that all sockets on the connectors were properly connected to the respective banana jack.

When compared to the Gold Box BOBs, the new BOB has many advantages. It is much more cost efficient, it delivers equal usability at substantially lower cost of the BOB, and the Gold Box is much heavier when compared to the new BOB. The new BOB is also a bit longer and much more versatile in that connectors are easily changeable and if a banana jack is broken, it can be replaced instead of throwing away an entire BOB.

This work was done by Jason H. Lee of Caltech for NASA's Jet Propulsion Laboratory. For more information, contact iaoffice@jpl.nasa.gov. NPO-46799

Multiple-Beam Detection of Fast Transient Radio Sources

NASA's Jet Propulsion Laboratory, Pasadena, California

A method has been designed for using multiple independent stations to discriminate fast transient radio sources from local anomalies, such as antenna noise or radio frequency interference (RFI). This can improve the sensitivity of

incoherent detection for geographically separated stations such as the very long baseline array (VLBA), the future square kilometer array (SKA), or any other coincident observations by multiple separated receivers.

The transients are short, broadband pulses of radio energy, often just a few milliseconds long, emitted by a variety of exotic astronomical phenomena. They generally represent rare, high-energy events making them of great

scientific value. For RFI-robust adaptive detection of transients, using multiple stations, a family of algorithms has been developed. The technique exploits the fact that the separated stations constitute statistically independent samples of the target. This can be used to adaptively ignore RFI events for superior sensitivity. If the antenna signals are independent and identically distributed (IID), then RFI events are simply outlier data points that can be removed through robust estimation such as a trimmed or Winsorized estimator.

The alternative “trimmed” estimator is considered, which excises the strongest n signals from the list of short-beamed intensities. Because local RFI is independent at each antenna, this interference is unlikely to occur at many antennas on the same step. Trimming the strongest signals provides robustness to RFI that can theoretically outperform even the detection performance of the same number of antennas at a single site. This algorithm requires sorting the signals at each time step and dispersion measure, an operation that is computationally tractable for existing array sizes.

An alternative uses the various stations to form an ensemble estimate of the conditional density function (CDF) evaluated at each time step. Both methods outperform standard detection strategies on a test sequence of VLBA data, and both are efficient enough for deployment in real-time, online transient detection applications.

This work was done by David R. Thompson, Kiri L. Wagstaff, and Walid A. Majid of Caltech for NASA's Jet Propulsion Laboratory. Further information is contained in a TSP (see page 1). NPO-47678

Router Agent Technology for Policy-Based Network Management

NASA's Jet Propulsion Laboratory, Pasadena, California

This innovation can be run as a stand-alone network application on any computer in a networked environment. This design can be configured to control one or more routers (one instance per router), and can also be configured to listen to a policy server over the network to receive new policies based on the policy-based network management technology. The Router Agent Technology transforms the received policies into suitable Access Control List syntax for the routers it is configured to control. It commits the newly generated access control lists to the routers and provides feedback regarding any errors that were

faced. The innovation also automatically generates a time-stamped log file regarding all updates to the router it is configured to control.

This technology, once installed on a local network computer and started, is autonomous because it has the capability to keep listening to new policies from the policy server, transforming those policies to router-compliant access lists, and committing those access lists to a specified interface on the specified router on the network with any error feedback regarding commitment process.

The stand-alone application is named RouterAgent and is currently realized as

a fully functional (version 1) implementation for the Windows operating system and for CISCO routers.

This work was done by Edward T. Chow, Gurusham Sudhir, Hsin-Ping Chang, Mark James, and Yih-Chiao J. Liu of Caltech and Winston Chiang of the University of Southern California for NASA's Jet Propulsion Laboratory. Further information is contained in a TSP (see page 1).

The software used in this innovation is available for commercial licensing. Please contact Daniel Broderick of the California Institute of Technology at danielb@caltech.edu. Refer to NPO-47228.



Remote Asynchronous Message Service Gateway

The Remote Asynchronous Message Service (RAMS) gateway is a special-purpose AMS application node that enables exchange of AMS messages between nodes residing in different AMS “continua,” notionally in different geographical locations. JPL’s implementation of RAMS gateway functionality is integrated with the ION (Interplanetary Overlay Network) implementation of the DTN (Delay-Tolerant Networking) bundle protocol, and with JPL’s implementation of AMS itself. RAMS protocol data units are encapsulated in ION bundles and are forwarded to the neighboring RAMS gateways identified in the source gateway’s AMS management information base.

Each RAMS gateway has interfaces in two communication environments: the AMS message space it serves, and the RAMS network — the grid or tree of mutually aware RAMS gateways — that enables AMS messages produced in one message space to be forwarded to other message spaces of the same venture. Each gateway opens persistent, private RAMS network communication channels to the RAMS gateways of other message spaces for the same venture, in other continua. The interconnected RAMS gateways use these communication channels to forward message petition assertions and cancellations among themselves. Each RAMS gateway subscribes locally to all subjects that are of interest in any of the linked message spaces. On receiving its copy of a message on any of these subjects, the RAMS gateway node uses the RAMS network to forward the message to every other RAMS gateway whose message space contains at least one node that has subscribed to messages on that subject. On receiving a message via the RAMS network from some other RAMS gateway, the RAMS gateway node forwards the message to all subscribers in its own message space.

In this way, the RAMS protocol enables the free flow of published application messages across arbitrarily long, deep space links while protecting efficient use of those links: only a single copy of any message is ever transmitted on any RAMS network communication channel,

no matter how many subscribers will receive copies when the message reaches its destination message space.

Note that the nature of the RAMS network communication channels depends on the implementation of the RAMS network. In order to communicate over the RAMS network for a given venture, each RAMS gateway must know the RAMS network location — an endpoint in the protocol used to implement the RAMS network (e.g., the DTN bundle protocol) — at which every other RAMS gateway for that venture receives RAMS network traffic. Again, this extension of the publish/subscribe model to interplanetary communications is invisible to application nodes. Application functionality is unaffected by these details of network configuration, and the only effects on behavior are those that are intrinsic to variability in message propagation latency.

This work was done by Shin-Ywan Wang of Caltech and Scott C. Burleigh of SBAR for NASA’s Jet Propulsion Laboratory. Further information is contained in a TSP (see page 1).

This software is available for commercial licensing. Please contact Daniel Broderick of the California Institute of Technology at danielb@caltech.edu. Refer to NPO-44048.

Automatic Tie Pointer for In-Situ Pointing Correction

The MARSAUTOTIE program generates tie points for use with the Mars pointing correction software “In-Situ Pointing Correction and Rover Microlocalization,” (NPO-46696) *Software Tech Briefs*, Vol. 34, No. 9 (September 2010), page 18, in a completely automated manner, with no operator intervention. It takes the place of MARSTIE, although MARSTIE can be used to interactively edit the tie points afterwards. These tie points are used to create a mosaic whose seams (boundaries of input images) have been geometrically corrected to reduce or eliminate errors and misregistrations. The methods used to find appropriate tie points for use in creating a mosaic are unique, having been designed to work in concert with the “MARSNAV” program to be most effective in reducing or eliminating geometric seams in a mosaic.

The program takes the input images and finds overlaps according to the

nominal pointing. It then finds the most interesting areas using a scene activity metric. Points with higher scene activity are more likely to correlate successfully in the next step. It then uses correlation techniques to find matching points in the overlapped image. Finally, it performs a series of steps to reduce the number of tie points to a manageable level. These steps incorporate a number of heuristics that have been devised using experience gathered by tie pointing mosaics manually during MER operations. The software makes use of the PIG library as described in “Planetary Image Geometry Library” (NPO-46658), *NASA Tech Briefs*, Vol. 34, No. 12 (December 2010), page 30, so it is multi-mission, applicable without change to any *in-situ* mission supported by PIG.

The MARSAUTOTIE algorithm is automated, so it requires no user intervention. Although at the time of this reporting it has not been done, this program should be suitable for integration into a fully automated mosaic production pipeline.

This work was done by Robert G. Deen of Caltech for NASA’s Jet Propulsion Laboratory. For more information, contact iaoffice@jpl.nasa.gov.

This software is available for commercial licensing. Please contact Daniel Broderick of the California Institute of Technology at danielb@caltech.edu. Refer to NPO-47083.

Jitter Correction

Jitter_Correct.m is a MATLAB function that automatically measures and corrects inter-frame jitter in an image sequence to a user-specified precision. In addition, the algorithm dynamically adjusts the image sample size to increase the accuracy of the measurement.

The Jitter_Correct.m function takes an image sequence with unknown frame-to-frame jitter and computes the translations of each frame (column and row, in pixels) relative to a chosen reference frame with sub-pixel accuracy. The translations are measured using a Cross Correlation Fourier transformation method in which the relative phase of the two transformed images is fit to a plane. The measured translations are then used to correct the inter-frame jitter of the image sequence. The function also dynamically expands the image sam-

ple size over which the cross-correlation is measured to increase the accuracy of the measurement. This increases the robustness of the measurement to variable magnitudes of inter-frame jitter.

This work was done by Mordecai J. Waegell and David M. Palacios of Caltech for NASA's Jet Propulsion Laboratory. For more information, contact iaoffice@jpl.nasa.gov.

This software is available for commercial licensing. Please contact Daniel Broderick of the California Institute of Technology at danielb@caltech.edu. Refer to NPO-47215.

MSLICE Sequencing

MSLICE Sequencing is a graphical tool for writing sequences and integrating them into RML files, as well as for producing SCMF files for uplink. When operated in a testbed environment, it also supports uplinking these SCMF files to the testbed via Chill.

This software features a freeform textual sequence editor featuring syntax coloring, automatic content assistance (including command and argument completion proposals), complete with types, value ranges, unites, and descriptions from the command dictionary that appear as they are typed. The sequence editor also has a "field mode" that allows tabbing between arguments and displays type/range/units/description for each argument as it is edited. Color-coded error and warning annotations on problematic tokens are included, as well as indications of problems that are not visible in the current scroll range. "Quick Fix" suggestions are made for resolving problems, and all the features afforded by modern source editors are also included such as copy/cut/paste, undo/redo, and a sophisticated find-and-replace system optionally using regular expressions.

The software offers a full XML editor for RML files, which features syntax coloring, content assistance and problem annotations as above. There is a form-based, "detail view" that allows structured editing of command arguments and sequence parameters when preferred. The "project view" shows the user's "workspace" as a tree of "resources" (projects, folders, and files) that can subsequently be opened in editors by double-clicking.

Files can be added, deleted, dragged-dropped/copied-pasted between folders or projects, and these operations are undoable and redoable.

A "problems view" contains a tabular list of all problems in the current workspace. Double-clicking on any row in the table opens an editor for the appropriate sequence, scrolling to the specific line with the problem, and highlighting the problematic characters. From there, one can invoke "quick fix" as described above to resolve the issue. Once resolved, saving the file causes the problem to be removed from the problem view.

This work was done by Thomas M. Crockett, Joseph C. Joswig, Khawaja S. Shams, Jeffrey S. Norris, and John R. Morris of Caltech for NASA's Jet Propulsion Laboratory. For more information, contact iaoffice@jpl.nasa.gov.

This software is available for commercial licensing. Please contact Daniel Broderick of the California Institute of Technology at danielb@caltech.edu. Refer to NPO-47292.

EOS MLS Level 2 Data Processing Software Version 3

This software accepts the EOS MLS calibrated measurements of microwave radiances products and operational meteorological data, and produces a set of estimates of atmospheric temperature and composition. This version has been designed to be as flexible as possible. The software is controlled by a Level 2 Configuration File that controls all aspects of the software: defining the contents of state and measurement vectors, defining the configurations of the various forward models available, reading appropriate *a priori* spectroscopic and calibration data, performing retrievals, post-processing results, computing diagnostics, and outputting results in appropriate files.

In production mode, the software operates in a parallel form, with one instance of the program acting as a master, coordinating the work of multiple slave instances on a cluster of computers, each computing the results for individual chunks of data. In addition, to do conventional retrieval calculations and producing geophysical products, the Level 2 Configuration File can instruct

the software to produce files of simulated radiances based on a state vector formed from a set of geophysical product files taken as input. Combining both the retrieval and simulation tasks in a single piece of software makes it far easier to ensure that identical forward model algorithms and parameters are used in both tasks. This also dramatically reduces the complexity of the code maintenance effort.

This work was done by Nathaniel J. Livesey, W. Van Snyder, William G. Read, Michael J. Schwartz, Alyn Lambert, Michelle L. Santee, Honghanh T. Nguyen, Lucien Froidevaux, Shuhui Wang, Gloria L. Manney, Dong L. Wu, and Paul A. Wagner of Caltech; Christina Vuu of Raytheon; and Hugh C. Pumphrey of the University of Edinburgh for NASA's Jet Propulsion Laboratory. For more information, contact iaoffice@jpl.nasa.gov.

This software is available for commercial licensing. Please contact Daniel Broderick of the California Institute of Technology at danielb@caltech.edu. Refer to NPO-47221.

DspaceOgre 3D Graphics Visualization Tool

This general-purpose 3D graphics visualization C++ tool is designed for visualization of simulation and analysis data for articulated mechanisms. Examples of such systems are vehicles, robotic arms, biomechanics models, and biomolecular structures. DspaceOgre builds upon the open-source Ogre3D graphics visualization library. It provides additional classes to support the management of complex scenes involving multiple viewpoints and different scene groups, and can be used as a remote graphics server.

This software provides improved support for adding programs at the graphics processing unit (GPU) level for improved performance. It also improves upon the messaging interface it exposes for use as a visualization server.

This work was done by Abhinandan Jain, Steven Myint, and Marc I. Pomerantz of Caltech for NASA's Jet Propulsion Laboratory. For more information, contact iaoffice@jpl.nasa.gov.

This software is available for commercial licensing. Please contact Daniel Broderick of the California Institute of Technology at danielb@caltech.edu. Refer to NPO-47380.



Metallization for $\text{Yb}_{14}\text{MnSb}_{11}$ -Based Thermoelectric Materials

Process enables device fabrication using advanced, high-temperature thermoelectric material.

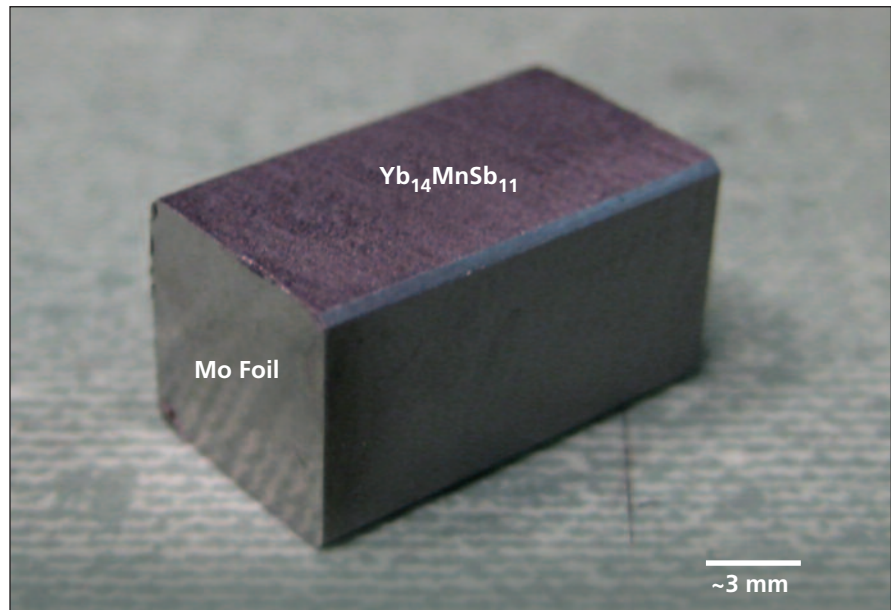
NASA's Jet Propulsion Laboratory, Pasadena, California

Thermoelectric materials provide a means for converting heat into electrical power using a fully solid-state device. Power-generating devices (which include individual couples as well as multi-couple modules) require the use of n-type and p-type thermoelectric materials, typically comprising highly doped narrow band-gap semiconductors which are connected to a heat collector and electrodes.

To achieve greater device efficiency and greater specific power will require using new thermoelectric materials, in more complex combinations. One such material is the p-type compound semiconductor $\text{Yb}_{14}\text{MnSb}_{11}$ (YMS), which has been demonstrated to have one of the highest ZT values at 1,000 °C, the desired operational temperature of many space-based radioisotope thermoelectric generators (RTGs).

Despite the favorable attributes of the bulk YMS material, it must ultimately be incorporated into a power-generating device using a suitable joining technology. Typically, processes such as diffusion bonding and/or brazing are used to join thermoelectric materials to the heat collector and electrodes, with the goal of providing a stable, ohmic contact with high thermal conductivity at the required operating temperature.

Since YMS is an inorganic compound featuring chemical bonds with a mixture of covalent and ionic character, simple metallurgical diffusion bonding is difficult to implement. Furthermore, the Sb within YMS readily reacts with most metals to form antimonide compounds with a wide range of stoichiometries. Although choosing metals that react to form high-melting-point antimonides could be employed to form a stable reaction bond, it is difficult to limit the reactivity of Sb in YMS such that the electrode is not completely consumed at an operating temperature of 1,000 °C. Previous attempts to form suitable metallization layers resulted in poor bonding, complete consumption of the metallization layer or fracture within the YMS thermoelement (or leg).



Metallized $\text{Yb}_{14}\text{MnSb}_{11}$ Leg, terminated on both ends with Mo layers.

An approach to forming a stable metallization layer to consolidated YMS parts or legs has been developed, however, using thin molybdenum foils. The foil is diffusion bonded to the YMS part at temperatures above 900 °C, under the application of adequate pressure for several hours. Use of a thin foil eliminates the fracture typically observed within YMS parts when thicker foils are used (induced by thermo-mechanical stresses) as seen in the figure. The metal can be bonded prior to dicing of the legs from a hot-pressed/consolidated YMS form, or it can be bonded to a pre-cut leg of the correct geometry. The contact is thermally stable with respect to YMS, exhibiting no de-bonding or increase in contact resistance after a 1,000 °C vacuum heat treatment for 1,500 hours. This metallization layer may then be bonded or brazed to other components, such as heat collectors or current-carrying electrodes. To enable successful bonding of the molybdenum metallization requires the preparation of YMS legs of sufficient strength, which is facilitated by the hot pressing of YMS powders above 900 °C (using proper cooling

rates to minimize residual stress formation and avoid fracture of the parts).

This metallization layer may then be bonded or brazed to other components, such as heat collectors or current-carrying electrodes. Furthermore, it can be implemented at both the hot and cold sides of the leg. It can also be applied as a metallization layer to other similar compositions of thermoelectric materials. The specific nature of the interaction between Mo and YMS is still under investigation; however, it is clear the molybdenum reacts sufficiently to form an adequate bond, without the extensive reaction observed with similar metals such as nickel, niobium, or titanium. The process may be similar to that involved in the formation of other metal/ceramic bonds, wherein the metal has limited solubility in the ceramic material (for example, in diffusion bonded metal/alumina joints).

This work was done by Samad Firdosy, Billy Chun-Yip Li, Vilupanur Ravi, Jeffrey Sakamoto, Thierry Caillat, Richard C. Ewell, and Erik J. Brandon of Caltech for NASA's Jet Propulsion Laboratory. Further information is contained in a TSP (see page 1). NPO-46670

Solvent/Non-Solvent Sintering To Make Microsphere Scaffolds

Lyndon B. Johnson Space Center, Houston, Texas

A solvent/non-solvent sintering technique has been devised for joining polymeric microspheres to make porous matrices for use as drug-delivery devices or scaffolds that could be seeded with cells for growing tissues. Unlike traditional sintering at elevated temperature and pressure, this technique is practiced at room temperature and pressure and, therefore, does not cause thermal degradation of any drug, protein, or other biochemical with which the microspheres might be loaded to

impart properties desired in a specific application. Also, properties of scaffolds made by this technique are more reproducible than are properties of comparable scaffolds made by traditional sintering.

The technique involves the use of two miscible organic liquids: one that is and one that is not a solvent for the affected polymer. The polymeric microspheres are placed in a mold having the size and shape of the desired scaffold, then the solvent/non-solvent mixture is poured

into the mold to fill the void volume between the microspheres, then the liquid mixture is allowed to evaporate. Some of the properties of the resulting scaffold can be tailored through choice of the proportions of the liquids and the diameter of the microspheres.

This work was done by Cato T. Laurencin, Justin L. Brown, and Lakshmi Nair of the University of Virginia for Johnson Space Center. For further information, contact the Johnson Technology Transfer Office at (281) 483-3809. MSC-24227-1



Enhanced Fuel-Optimal Trajectory-Generation Algorithm for Planetary Pinpoint Landing

Enhancements are incorporated to allow faster convergence to the fuel optimal solution.

NASA's Jet Propulsion Laboratory, Pasadena, California

An enhanced algorithm is developed that builds on a previous innovation of fuel-optimal powered-descent guidance (PDG) for planetary pinpoint landing. The PDG problem is to compute constrained, fuel-optimal trajectories to land a craft at a prescribed target on a planetary surface, starting from a “parachute cut-off” point and using a throttleable descent engine. The previous innovation showed the minimal-fuel PDG problem can be posed as a convex optimization problem, in particular, as a Second-Order Cone Program, which can be solved to global optimality with deterministic convergence properties, and hence is a candidate for onboard implementation. To increase the speed and robustness of this convex PDG algorithm for possible onboard implementation, the following enhancements are incorporated:

- Fast detection of infeasibility (i.e., control authority is not sufficient for soft-landing) for subsequent fault response.

- The use of a piecewise-linear control parameterization, providing smooth solution trajectories and increasing computational efficiency.
- An enhanced line-search algorithm for optimal time-of-flight, providing quicker convergence and bounding the number of path-planning iterations needed.
- An additional constraint that analytically guarantees inter-sample satisfaction of glide-slope and non-sub-surface flight constraints, allowing larger discretizations and, hence, faster optimization.
- Explicit incorporation of Mars rotation rate into the trajectory computation for improved targeting accuracy.

These enhancements allow faster convergence to the fuel-optimal solution and, more importantly, remove the need for a “human-in-the-loop,” as constraints will be satisfied over the entire path-planning interval independent of step-size (as opposed to just at the discrete

time points) and infeasible initial conditions are immediately detected. Finally, while the PDG stage is typically only a few minutes, ignoring the rotation rate of Mars can introduce 10s of meters of error. By incorporating it, the enhanced PDG algorithm becomes capable of pinpoint targeting.

This work was done by Behcet Acikmese, James C. Blackmore, and Daniel P. Scharf of Caltech for NASA's Jet Propulsion Laboratory. For more information, contact iaoffice@jpl.nasa.gov.

In accordance with Public Law 96-517, the contractor has elected to retain title to this invention. Inquiries concerning rights for its commercial use should be addressed to:

*Innovative Technology Assets Management
JPL*

*Mail Stop 202-233
4800 Oak Grove Drive
Pasadena, CA 91109-8099*

E-mail: iaoffice@jpl.nasa.gov

Refer to NPO-46648, volume and number of this NASA Tech Briefs issue, and the page number.



Self-Cleaning Coatings and Materials for Decontaminating Field-Deployable Land and Water-Based Optical Systems

Stennis Space Center, Mississippi

This technology exploits the organic decomposition capability and hydrophilic properties of the photocatalytic material titanium dioxide (TiO₂), a non-toxic and non-hazardous substance, to address contamination and biofouling issues in field-deployed optical sensor systems. Specifically, this technology incorporates TiO₂ coatings and materials applied to, or integrated as a part of, the optical surfaces of sensors and calibration sources, including lenses, windows, and mirrors that are used in remote, unattended, ground-based (land or maritime) optical sensor systems.

Current methods used to address contamination or biofouling of these optical surfaces in deployed systems are costly, toxic, labor intensive, and non-preventative. By implementing this novel technology, many of these negative aspects can be reduced. The functionality of this

innovative self-cleaning solution to address the problem of contamination or biofouling depends on the availability of a sufficient light source with the appropriate spectral properties, which can be attained naturally via sunlight or supplemented using artificial illumination such as UV LEDs (light emitting diodes).

In land-based or above-water systems, the TiO₂ optical surface is exposed to sunlight, which catalyzes the photocatalytic reaction, facilitating both the decomposition of inorganic and organic compounds, and the activation of superhydrophilic properties. Since underwater optical surfaces are submerged and have limited sunlight exposure, supplementary UV light sources would be required to activate the TiO₂ on these optical surfaces. Nighttime operation of land-based or above-water systems would require this addition as well. For most superhy-

drophilic self-cleaning purposes, a rainwater wash will suffice; however, for some applications an attached rainwater collector/dispenser or other fresh water dispensing system may be required to wash the optical surface and initiate the removal of contaminants. Deployment of this non-toxic, non-hazardous technology will take advantage of environmental elements (i.e. rain and sunlight), increase the longevity of unattended optical systems, increase the amount of time between required maintenance, and improve the long-term accuracy of sensor measurements.

This work was done by Robert Ryan, Lauren Underwood, and Kara Holekamp of Science Systems and Applications, Inc., George May of Institute of Technology Development, and Bruce Spiering and Bruce Davis of Stennis Space Center. For more information contact Robert Ryan at (228) 688-2276. Refer to SSC-00303.

Separation of Single-Walled Carbon Nanotubes with DEP-FFF

Simultaneous type and diameter separation of SWNTs is achieved by using flow injection dielectrophoresis.

Lyndon B. Johnson Space Center, Houston, Texas

A process using a modified dielectrophoresis device separates single-walled carbon nanotubes (SWNTs) according to their polarizability in electric fields. This depends on the size and dielectric constant of individual nanotubes and easily separates metallic from semiconducting nanotubes. Separation by length has also been demonstrated. Partial separation (enrichment) according to bandgap (which is linked to polarizability) has also been shown and can be improved to full separation of individual types of semiconducting SWNTs with better control over operational parameters and the length of SWNT starting material. This process and device can be scaled affordably to generate useful amounts of semiconducting SWNTs for electronic device development and production.

In this study, a flow injection dielectrophoresis technique was used with a modified dielectrophoresis device. The length, width, and height of the modified chamber were 28, 2.5, and 0.025 cm, respectively. On the bottom of the chamber, there are two arrays of 50- μ m-wide, 2- μ m-thick gold electrodes, which are connected to an AC voltage generator and are alternately arranged so that every electrode is adjacent to two electrodes of the opposite polar. There is an additional plate electrode on the top of the chamber that is negatively biased.

During the experiment, a syringe pump constantly pumps in the mobile phase, 1-percent sodium dodecylbenzene sulfonate (SDBS) solution, into the chamber. The frequency and voltage are set to 1 MHz and 10 V peak-to-peak, re-

spectively. About 150 μ L of SWNTs in 1-percent SDBS decanted solution are injected to the mobile phase through a septum near the entrance of the chamber. The flow rate of the mobile phase is set to 0.02 cm³/min. The injected SWNTs sample flows through the chamber before it is lead into a fluorescence flow-through cell and collected for further analysis. The flow-through cell has three windows, thus allowing the fluorometer to collect fluorescence spectrum and visible absorption spectrums simultaneously.

Dielectrophoresis field-flow fractionation (DEP-FFF) generally depends on interaction of a sedimentation force and DEP force for particle separation, and SWNTs are neutrally buoyant in water. In this innovation, the third electrode was added to create a sedi-

mentation force based on DC electrophoresis. This makes this particular device applicable to separations on any neutrally buoyant particles in solution and a more general process for a broad range of nanomaterials sorting and separations.

This work was done by Howard K. Schmidt, Haiqing Peng, Noe Alvarez, Manuel Mendes,

and Matteo Pasquali of Rice University for Johnson Space Center. For further information, contact the JSC Innovation Partnerships Office at (281) 483-3809.

In accordance with Public Law 96-517, the contractor has elected to retain title to this invention. Inquiries concerning rights for its commercial use should be addressed to:

*Rice University
Office of Technology Transfer—MS 705
P.O. Box 1892
Houston, TX 77005
Phone No.: (713) 348-6188
E-mail: techtran@rice.edu*

Refer to MSC-24368-1/70-1, volume and number of this NASA Tech Briefs issue, and the page number.

Li Anode Technology for Improved Performance

John H. Glenn Research Center, Cleveland, Ohio

A novel, low-cost approach to stabilization of Li metal anodes for high-performance rechargeable batteries was developed. Electrolyte additives are selected and used in Li cell electrolyte systems, promoting formation of a protective coating on Li metal anodes for improved cycle and safety performance.

Li batteries developed from the new system will show significantly improved battery performance characteristics, including energy/power density, cycle/calendar life, cost, and safety.

This work was done by Tuqiang Chen of TH Chem for Glenn Research Center. Further information is contained in a TSP (see page 1).

Inquiries concerning rights for the commercial use of this invention should be addressed to NASA Glenn Research Center, Innovative Partnerships Office, Attn: Steven Fedor, Mail Stop 4-8, 21000 Brookpark Road, Cleveland, Ohio 44135. Refer to LEW-18715-1.



Post-Fragmentation Whole Genome Amplification-Based Method

This method has application in hospital cleanliness validation assays, pharmaceutical development, and medical device manufacturing and packaging.

NASA's Jet Propulsion Laboratory, Pasadena, California

This innovation is derived from a proprietary amplification scheme that is based upon random fragmentation of the genome into a series of short, overlapping templates. The resulting shorter DNA strands (<400 bp) constitute a library of DNA fragments with defined 3' and 5' termini. Specific primers to these termini are then used to isothermally amplify this library into potentially unlimited quantities that can be used immediately for multiple downstream applications including gel electrophoresis, quantitative polymerase chain reaction (QPCR), comparative genomic hybridization microarray, SNP analysis, and sequencing.

The standard reaction can be performed with minimal hands-on time, and can produce amplified DNA in as little as three hours. Post-fragmentation whole genome amplification-based technology provides a robust and accurate method of amplifying femtogram levels of starting material into microgram yields with no detectable allele bias. The amplified DNA also facilitates the preservation of samples (spacecraft samples) by amplifying scarce amounts of template DNA into microgram concen-

trations in just a few hours. Based on further optimization of this technology, this could be a feasible technology to use in sample preservation for potential future sample return missions.

The research and technology development described here can be pivotal in dealing with backward/forward biological contamination from planetary missions. Such efforts rely heavily on an increasing understanding of the burden and diversity of microorganisms present on spacecraft surfaces throughout assembly and testing.

The development and implementation of these technologies could significantly improve the comprehensiveness and resolving power of spacecraft-associated microbial population censuses, and are important to the continued evolution and advancement of planetary protection capabilities. Current molecular procedures for assaying spacecraft-associated microbial burden and diversity have inherent sample loss issues at practically every step, particularly nucleic acid extraction. In engineering a molecular means of amplifying nucleic acids directly from single cells in their native

state within the sample matrix, this innovation has circumvented entirely the need for DNA extraction regimes in the sample processing scheme.

As typically 90 percent of the biomaterial held within a sample is lost at the extraction step, the absence of DNA extraction in processing a sample of low biomass is quite appealing and seemingly superior, at least in theory. If current understanding of spacecraft-associated microbial burden/diversity is based on a mere 10% of the actual sample collected, then a much broader diversity and elevated bioburden should be able to be resolved upon mitigating this ~ 90% loss of sample biomatter. This innovative process should lend considerable credence to such assays, and ultimately result in a much more comprehensive knowledge base of the abundance and phylogenetic diversity of microbes on and around spacecraft surfaces.

This work was done by James (Nick) Benardini and Myron T. La Duc of Caltech and John Langmore of Rubicon Genomics for NASA's Jet Propulsion Laboratory. For more information, contact iaoffice@jpl.nasa.gov. NPO-47201

Microwave Tissue Soldering for Immediate Wound Closure

Wounds can be closed rapidly, without staples, sutures, or tapes.

Lyndon B. Johnson Space Center, Houston, Texas

A novel approach for the immediate sealing of traumatic wounds is under development. A portable microwave generator and handheld antenna are used to seal wounds, binding the edges of the wound together using a biodegradable protein sealant or "solder." This method could be used for repairing wounds in emergency settings by restoring the wound surface to its original strength within minutes. This technique could also be utilized for surgical purposes involving solid visceral organs

(i.e., liver, spleen, and kidney) that currently do not respond well to ordinary surgical procedures.

A miniaturized microwave generator and a handheld antenna are used to deliver microwave energy to the protein solder, which is applied to the wound. The antenna can be of several alternative designs optimized for placement either in contact with or in proximity to the protein solder covering the wound. In either case, optimization of the de-

sign includes the matching of impedances to maximize the energy delivered to the protein solder and wound at a chosen frequency. For certain applications, an antenna could be designed that would emit power only when it is in direct contact with the wound.

The optimum frequency or frequencies for a specific application would depend on the required depth of penetration of the microwave energy. In fact, a computational simulation for each spe-

cific application could be performed, which would then match the characteristics of the antenna with the protein solder and tissue to best effect wound closure. An additional area of interest with potential benefit that remains to be validated is whether microwave energy can effectively kill bacteria in and around the wound. Thus, this may be an efficient method for simultaneously sterilizing and closing wounds.

Using microwave energy to seal wounds has a number of advantages over lasers, which are currently in experimental use in some hospitals. Laser tissue welding is unsuitable for emergency use because its large, bulky equipment cannot be easily moved between operat-

ing rooms, let alone relocated to field sites where emergencies often occur. In addition, this approach is highly dependent on the uniformity and thickness of the protein solder as well as the surgeon's skills. In contrast, the use of microwave energy is highly tolerant of the thickness of the protein solder, level of fluids in and around the wound, and other parameters that can adversely affect the outcome of laser welding. However, controlling the depth of penetration of the microwave energy into the wound is critical for achieving effective wound sealing without damaging the adjacent tissue. In addition, microspheres that encapsulate metallic cores could also be incorporated into the protein

solder to further control the depth of penetration of the microwave energy.

This work was performed by G. Dickey Arndt, Phong H. Ngo, Chau T. Phan, and Diane Byerly of Johnson Space Center; John Dosl of Jacobs Sverdrup; Marguerite A. Sognier of Universities Space Research Association; and Jim Carl of Advanced Electromagnetics. For further information, contact the JSC Innovation Partnerships Office at (281) 483-3809.

This invention is owned by NASA, and a patent application has been filed. Inquiries concerning nonexclusive or exclusive license for its commercial development should be addressed to the Patent Counsel, Johnson Space Center, (281) 483-1003. Refer to MSC-24238-1.

Principles, Techniques, and Applications of Tissue Microfluidics

This technique can be used in the diagnosis of diseases such as cancer.

NASA's Jet Propulsion Laboratory, Pasadena, California

The principle of tissue microfluidics and its resultant techniques has been applied to cell analysis. Building microfluidics to suit a particular tissue sample would allow the rapid, reliable, inexpensive, highly parallelized, selective extraction of chosen regions of tissue for purposes of further biochemical analysis. Furthermore, the applicability of the techniques ranges beyond the described pathology application. For example, they would also allow the posing and successful answering of new sets of questions in many areas of fundamental research.

The proposed integration of microfluidic techniques and tissue slice samples is called "tissue microfluidics" because it molds the microfluidic architectures in accordance with each particular structure of each specific tissue sample. Thus, microfluidics can be built around the tissues, following the tissue structure, or alternatively, the microfluidics can be adapted to the specific geometry of particular tissues. By contrast, the traditional approach is that microfluidic devices are structured in accordance with engineering considerations, while the biological components in applied devices are forced to comply with these engineering presets.

The proposed principles represent a paradigm shift in microfluidic technol-

ogy in three important ways:

- Microfluidic devices are to be directly integrated with, onto, or around tissue samples, in contrast to the conventional method of off-chip sample extraction followed by sample insertion in microfluidic devices.
- Architectural and operational principles of microfluidic devices are to be subordinated to suit specific tissue structure and needs, in contrast to the conventional method of building devices according to fluidic function alone and without regard to tissue structure.
- Sample acquisition from tissue is to be performed on-chip and is to be integrated with the diagnostic measurement within the same device, in contrast to the conventional method of off-chip sample prep and subsequent insertion into a diagnostic device. A more advanced form of tissue integration with microfluidics is tissue encapsulation, wherein the sample is completely encapsulated within a microfluidic device, to allow for full surface access.

The immediate applications of these approaches lie with diagnostics of tissue slices and biopsy samples — e.g. for cancer — but the approaches would also be very useful in comparative genomics and other areas of fundamental research involving heterogeneous tissue samples.

The approach advocates and utilizes the bottom-up customization of microfluidic architectures to biosamples, in contrast to the traditional top-down approach of building the architectures first and then putting the biosamples inside. Further, as particular embodiments of the above principle, novel techniques of sub-sample selection and isolation are presented. These techniques would have wide applicability in fundamental research and biomedical diagnostics.

In particular, an *in situ* microfluidic technique of single-cell isolation, or multiple single-cell isolations, is described, and is performed upon tissue sections attached to pathology glass slides. The technique combines the advantages of preserving the architectural integrity of the tissue section while allowing flexibility and precision of cell selection, rapid prototyping, and enhanced sample purity, while benefiting from the experience of the pathologist in the selection process. The result is a system that would allow the rapid and reliable biochemical analysis and diagnosis of pathologic processes with sensitivity extended down to the level of even a single cell, with high levels of confidence in the diagnostic determination.

These techniques would allow the extraction of cells and cell nuclei chosen for their potentially pathologic origin,

e.g. cancer. The chief advantages of the proposed methods are their speed, ease, reliability, and capacity to select individual cells from a tissue slice population with a higher degree of purity and specificity. The result is the extracted DNA can be biochemically analyzed with a higher degree of diagnostic accuracy, as the isolated sub-sample would not be diluted by unwanted material from the ambient tissue. In comparison to other

techniques, the proposed methods would combine high specificity with high speed.

This work was done by Lawrence A. Wade of Caltech and Emil P. Kartalov, Darryl Shibata, and Clive Taylor of the University of Southern California for NASA's Jet Propulsion Laboratory. Further information is contained in a TSP (see page 1).

In accordance with Public Law 96-517, the contractor has elected to retain title to this

invention. Inquiries concerning rights for its commercial use should be addressed to:

*Innovative Technology Assets Management
JPL*

Mail Stop 202-233

4800 Oak Grove Drive

Pasadena, CA 91109-8099

E-mail: iaoffice@jpl.nasa.gov

Refer to NPO-47561, volume and number of this NASA Tech Briefs issue, and the page number.

Robotic Scaffolds for Tissue Engineering and Organ Growth

Biocompatible and biodegradable smart scaffolds could reconfigure their shape and size to accommodate organ development.

NASA's Jet Propulsion Laboratory, Pasadena, California

The aim of tissue engineering (TE) is to restore tissue and organ functions with minimal host rejection. TE is seen as a future solution to solve the crisis of donor organs for transplant, which faces a shortage expected only to increase in the future. In this innovation, a flexible and configurable scaffold has been conceived that mechanically stresses cells that are seeded on it, stimulating them to increased growth.

The influence of mechanical stress/loading on cell growth has been observed on all forms of cells. For example, for cartilages, studies in animals, tissue explants, and engineered tissue scaffolds have all shown that cartilage cells (chondrocytes) modify their extracellular matrix in response to loading. The chondrocyte EMC production re-

sponse to dynamics of the physical environment (*in vivo* cartilage development) illustrates a clear benefit (better growth) when stressed. It has been shown that static and dynamic compression regulates PRG4 biosynthesis by cartilage explants.

Mechanical tissue stimulation is beneficial and (flexible) scaffolds with movable components, which are able to induce mechanical stimulation, offer advantages over the fixed, rigid scaffold design. In addition to improved cell growth from physical/mechanical stimulation, additional benefits include the ability to increase in size while preserving shape, or changing shape.

By making scaffolds flexible, allowing relative movement between their components, adding sensing (e.g., for de-

tecting response of cells to drug release and to mechanical actions), building controls for drug release and movement, and building even simple algorithms for mapping sensing to action, these structures can actually be made into biocompatible and biodegradable robots. Treating them as robots is a perspective shift that may offer advantages in the design and exploitation of these structures of the future.

This work was done by Adrian Stoica of Caltech for NASA's Jet Propulsion Laboratory. For more information, contact iaoffice@jpl.nasa.gov.

This invention is owned by NASA, and a patent application has been filed. Inquiries concerning nonexclusive or exclusive license for its commercial development should be addressed to the Patent Counsel, NASA Management Office-JPL. Refer to NPO-47142.

Stress-Driven Selection of Novel Phenotypes

A methodology allows the experimental design of novel peptides and RNAs that have desired properties.

Lyndon B. Johnson Space Center, Houston, Texas

A process has been developed that can confer novel properties, such as metal resistance, to a host bacterium. This same process can also be used to produce RNAs and peptides that have novel properties, such as the ability to bind particular compounds. It is inherent in the method that the peptide or RNA will behave as expected in the target organism. Plasmid-born mini-gene libraries coding for either a population of combinatorial peptides or stable, artificial RNAs carrying random inserts are produced. These

libraries, which have no bias towards any biological function, are used to transform the organism of interest and to serve as an initial source of genetic variation for stress-driven evolution.

The transformed bacteria are propagated under selective pressure in order to obtain variants with the desired properties. The process is highly distinct from *in vitro* methods because the variants are selected in the context of the cell while it is experiencing stress. Hence, the selected peptide or RNA will,

by definition, work as expected in the target cell as the cell adapts to its presence during the selection process. Once the novel gene, which produces the sought phenotype, is obtained, it can be transferred to the main genome to increase the genetic stability in the organism. Alternatively, the cell line can be used to produce novel RNAs or peptides with selectable properties in large quantity for separate purposes. The system allows for easy, large-scale purification of the RNAs or peptide products.

The process has been reduced to practice by imposing sub-inhibitory concentrations of NiCl₂ on cells of the bacterium *Escherichia coli* that were transformed separately with the peptide library and RNA library. The evolved resistant clones were isolated, and sequences of the selected mini-gene variants were established. Clones resistant to NiCl₂ were found to carry identical plasmid variants with a functional mini-gene that specifically conferred significant nickel tolerance on the host cells. Sequencing of the selected mini-gene revealed a propensity of the encoded peptide to bind transient metal ions. Expression of the mini-gene markedly improved growth parameters of the

evolved clones at sub-inhibitory concentrations of NiCl₂ while being slightly detrimental in the absence of stress. Similar results have been obtained with the RNA libraries.

Overall, the results demonstrate a very natural outcome of the selection experiments in which the mini-genes were expected to be either successfully integrated into bacterial genetic networks, or rejected depending upon their effect on host fitness. This described approach can be useful as a laboratory model to study the dynamics of bacterial adaptive evolution on the molecular level. It can also provide a strategy for screening expressed DNA libraries in search of novel genes with desirable properties.

This work was done by George E. Fox, Victor G. Stepanov, and Yamei Liu of the University of Houston/College of Natural Sciences & Mathematics for Johnson Space Center.

In accordance with Public Law 96-517, the contractor has elected to retain title to this invention. Inquiries concerning rights for its commercial use should be addressed to:

*Office of Intellectual Property Management
University of Houston
316 E. Cullen
Houston, TX 77204-2015
Phone No.: (713) 743-9155
www.research.uh.edu*

Refer to MSC-24230-1, volume and number of this NASA Tech Briefs issue, and the page number.



Method for Accurately Calibrating a Spectrometer Using Broadband Light

John F. Kennedy Space Center, Florida

A novel method has been developed for performing very fine calibration of a spectrometer. This process is particularly useful for modern miniature charge-coupled device (CCD) spectrometers where a typical factory wavelength calibration has been performed and a finer, more accurate calibration is desired. Typically, the factory calibration is done with a spectral line source that generates light at known wavelengths, allowing specific pixels in the CCD array to be assigned wave-

length values. This method is good to about 1 nm across the spectrometer's wavelength range. This new method appears to be accurate to about 0.1 nm, a factor of ten improvement.

White light is passed through an unbalanced Michelson interferometer, producing an optical signal with significant spectral variation. A simple theory can be developed to describe this spectral pattern, so by comparing the actual spectrometer output against this predicted pattern, errors in the wavelength

assignment made by the spectrometer can be determined.

The primary unique feature of this innovation is its ability to calibrate every pixel across a given wavelength range as opposed to only calibrating a few pixels and interpolating the other values as is currently done.

This work was done by Stephen Simmons and Robert Youngquist of Kennedy Space Center. Further information is contained in a TSP (see page 1). KSC-13331

Catalytic Microtube Rocket Igniter

This device can also be used on commercial combustion devices such as furnaces, power generators, and gas-fueled cooking appliances like grills, ranges, and ovens.

John H. Glenn Research Center, Cleveland, Ohio

Devices that generate both high energy and high temperature are required to ignite reliably the propellant mixtures in combustion chambers like those present in rockets and other combustion systems. This catalytic microtube rocket igniter generates these conditions with a small, catalysis-based torch. While traditional spark plug systems can require anywhere from 50 W to multiple kW of power in different applications, this system has demonstrated ignition at less than 25 W. Reactants are fed to the igniter from the same tanks that feed the reactants to the rest of the rocket or combustion system. While this specific igniter was originally designed for liquid methane and liquid oxygen rockets, it can be easily operated with gaseous propellants or modified for hydrogen use in commercial combustion devices.

For the present cryogenic propellant rocket case, the main propellant tanks — liquid oxygen and liquid methane, respectively — are regulated and split into different systems for the individual stages of the rocket and igniter. As the catalyst requires a gas phase for reaction, either the stored boil-off of the tanks can be used directly or one stream each of

fuel and oxidizer can go through a heat exchanger/vaporizer that turns the liquid propellants into a gaseous form. For commercial applications, where the reactants are stored as gases, the system is simplified. The resulting gas-phase streams of fuel and oxidizer are then further divided for the individual components of the igniter.

One stream each of the fuel and oxidizer is introduced to a mixing bottle/apparatus where they are mixed to a fuel-rich composition with an O/F mass-based mixture ratio of under 1.0. This premixed flow then feeds into the catalytic microtube device. The total flow is on the order of 0.01 g/s. The microtube device is composed of a pair of sub-millimeter diameter platinum tubes connected only at the outlet so that the two outlet flows are parallel to each other. The tubes are each approximately 10 cm long and are heated via direct electric resistive heating. This heating brings the gasses to their minimum required ignition temperature, which is lower than the auto-thermal ignition temperature, and causes the onset of both surface and gas phase ignition producing hot temperatures and a highly

reacting flame.

The combustion products from the catalytic tubes, which are below the melting point of platinum, are injected into the center of another combustion stage, called the primary augments. The reactants for this combustion stage come from the same source but the flows of non-premixed methane and oxygen gas are split off to a secondary mixing apparatus and can be mixed in a near-stoichiometric to highly lean mixture ratio. The primary augments is a component that has channels venting this mixed gas to impinge on each other in the center of the augments, perpendicular to the flow from the catalyst. The total cross-sectional area of these channels is on a similar order as that of the catalyst. The augments has internal channels that act as a manifold to distribute equally the gas to the inward-venting channels. This stage creates a stable flame kernel as its flows, which are on the order of 0.01 g/s, are ignited by the combustion products of the catalyst. This stage is designed to produce combustion products in the flame kernel that exceed the auto-thermal ignition temperature of oxygen and methane.

While these combined components will mix and produce a near stoichiometric flame with a temperature high enough to ignite the reactants in most combustion devices, the overall mass flow rate and energy is still relatively low. For the extreme conditions of igniting a cryogenic propellant chemical rocket, this total may not be enough to maintain a flame in the adverse environment. To enable this operation, another gas phase stage called the secondary augments is added in series with the first two components. As more heat release is required, the mass flow rate is increased by an order of magnitude to more than 0.1 g/s for this stage. The flows are kept separate, however, until injected where they impinge and mix within this secondary augments. Again,

the flows are distributed via a manifold system then injected through ports that are sized more than an order of magnitude larger than the total port area of the first two components. The mixture is kept fuel rich so that the temperature is regulated below the melting point of the components. With the ignition of this stage, a large stable torch is produced to ignite the cryogenics.

The hardware is designed so that the total size of the device was similar to that of a traditional spark plug. Likewise, the outlet of the igniter mimics that of a spark plug in order to have it act as a direct replacement in combustion devices. In tests it functioned as such, lighting chambers with propellant flows an order of magnitude larger. Operation was demonstrated with back

pressures as low as 0.01 atmospheres up to approximately 10 atmospheres and in theory, these bounds could be wider. Ignition was demonstrated with reactant temperatures near chilled-in cryogenic conditions. This igniter serves as a low-energy alternative to spark ignition and can operate as an ignition source for a variety of commercial combustion devices.

This work was done by Steven J. Schneider and Matthew C. Deans of Glenn Research Center. Further information is contained in a TSP (see page 1).

Inquiries concerning rights for the commercial use of this invention should be addressed to NASA Glenn Research Center, Innovative Partnerships Office, Attn: Steven Fedor, Mail Stop 4-8, 21000 Brookpark Road, Cleveland, Ohio 44135. Refer to LEW-18565-1.

Stage Cylindrical Immersive Display

This collaborative design environment enables design engineers to be immersed in a car or airplane, for example, to evaluate the designs of components.

NASA's Jet Propulsion Laboratory, Pasadena, California

Panoramic images with a wide field of view intend to provide a better understanding of an environment by placing objects of the environment on one seamless image. However, understanding the sizes and relative positions of the objects in a panorama is not intuitive and prone to errors because the field of view is unnatural to human perception. Scientists are often faced with the difficult task of interpreting the sizes and relative positions of objects in an environment when viewing an image of the environment on computer monitors or prints. A panorama can display an object that appears to be to the right of the viewer when it is, in fact, behind the viewer. This misinterpretation can be very costly, especially when the environment is remote and/or only accessible by unmanned vehicles.

A 270° cylindrical display has been developed that surrounds the viewer with carefully calibrated panoramic imagery that correctly engages their natural kinesthetic senses and provides a more accurate awareness of the environment. The cylindrical immersive display offers a more natural window to the environment than a standard cubic CAVE (Cave Automatic Virtual Environment), and the geometry allows multiple collocated users to simultaneously view data and share important decision-making tasks.

A CAVE is an immersive virtual reality environment that allows one or more users to absorb themselves in a virtual environment. A common CAVE setup is a room-sized cube where the cube sides act as projection planes. By nature, all cubic CAVEs face a problem with edge matching at edges and corners of the display. Modern immersive displays have found ways to minimize seams by creating very tight edges, and rely on the user to ignore the seam. One significant deficiency of flat-walled CAVEs is that the sense of orientation and perspective within the scene is broken across adjacent walls. On any single wall, parallel lines properly converge at their vanishing point as they should, and the sense of perspective within the scene contained on only one wall has integrity. Unfortunately, parallel lines that lie on adjacent walls do not necessarily remain parallel. This results in inaccuracies in the scene that can distract the viewer and subtract from the immersive experience of the CAVE.

The cylindrical display overcomes the problem of distorted edges. Its smooth surface is perfectly equidistant from the viewer when he or she is positioned near the center. This eliminates the artifacts of a flat-walled CAVE where the viewing surface varies in distance from the viewer wherever he or she may stand

within it. The display is a curved rear-projected screen comprising three-quarters of a 12-ft-diameter (≈3.7-m-diameter) cylinder. The projection surface is a high-contrast, unity gain, flexible screen material. The screen is about 6.5 ft (≈2 m) tall, and the height of the actual image displayed on the screen is approximately 5 ft (≈1.5 m). A single consumer video card outputs to three short-throw projectors that are mounted behind the screen. Each projector illuminates 90° of the screen and overlaps slightly with an adjacent projector. The resolution of the entire cylindrical display is about 3,500×1,024 pixels. The projectors are edge-blended and calibrated into a seamless display using Scalable Display Technologies' camera-based calibration.

This system, known as Stage, is designed to address two critical visualization problems. First, people viewing imagery from surface spacecraft often incorrectly estimate the size of objects in the environment because imagery on a standard computer screen does not occupy the correct portion of their visual field. Second, people viewing panoramic images frequently fail to understand the relative positions of objects in the environment because the panoramic image is rolled out flat and presented in front of them instead of wrapping around them. These fundamental errors have well-documented and dramatic

consequences. Viewers frequently believe an object is beside a robot when it is actually behind it, or think that a small rock is actually a large, hazardous obstacle that must be avoided. Stage addresses both of

these problems by immersing viewers in an accurate representation of the operating environment.

This work was done by Lucy Abramyan, Jeffrey S. Norris, Mark W. Powell, David S.

Mittman, and Khawaja S. Shams of Caltech for NASA's Jet Propulsion Laboratory. For more information, contact iaoffice@jpl.nasa.gov. NPO-47469

Vacuum Camera Cooler

Cooler maintains proper operating temperature.

NASA's Jet Propulsion Laboratory, Pasadena, California

Acquiring cheap, moving video was impossible in a vacuum environment, due to camera overheating. This overheating is brought on by the lack of cooling media in vacuum. A water-jacketed camera cooler enclosure machined and assembled from copper plate and tube has been developed.

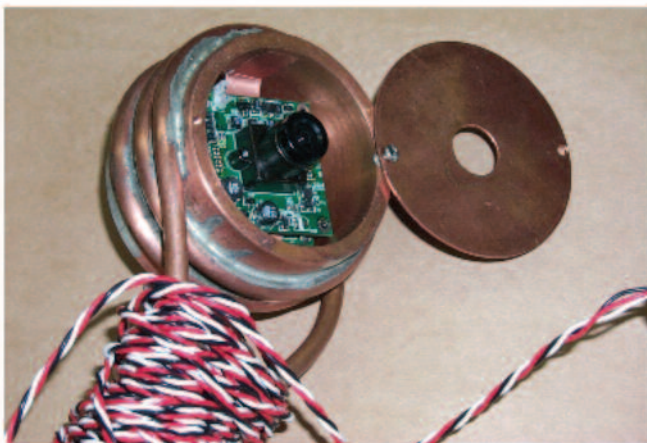
The camera cooler (see figure) is cup-shaped and cooled by circulating water or nitrogen gas through copper tubing.

The camera, a store-bought "spy type," is not designed to work in a vacuum. With some modifications the unit can be thermally connected when mounted in the cup portion of the camera cooler. The thermal conductivity is provided by copper tape between parts of the camera and the cooled enclosure.

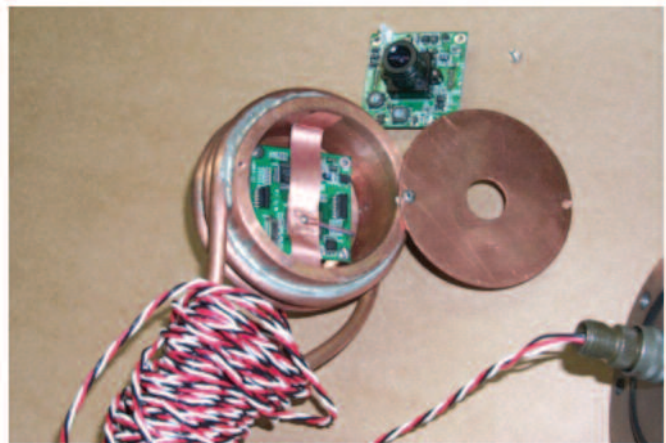
During initial testing of the demonstration unit, the camera cooler kept the

CPU (central processing unit) of this video camera at operating temperature. This development allowed video recording of an in-progress test, within a vacuum environment.

This work was performed by Geoffrey A. Laugen of Caltech for NASA's Jet Propulsion Laboratory. For more information, contact iaoffice@jpl.nasa.gov. NPO-47417



(a)



(b)

Photos of Vacuum Camera Cooler: (a) Camera cooler with camera installed and (b) camera cooler with camera partially removed to expose copper tape and thermocouple, which are attached to overheating camera CPU.

Atomic Oxygen Fluence Monitor

Applications include the semiconductor industry where atomic oxygen is used to clean and/or remove photoresist from semiconductor surfaces.

John H. Glenn Research Center, Cleveland, Ohio

This innovation enables a means for actively measuring atomic oxygen fluence (accumulated atoms of atomic oxygen per area) that has impinged upon spacecraft surfaces. Telemetered data from the device provides spacecraft designers, researchers, and mission managers with real-time measurement of atomic oxygen fluence, which is useful for prediction of the durability of spacecraft materials and components.

The innovation is a compact fluence measuring device that allows in-space measurement and transmittance of measured atomic oxygen fluence as a function of time based on atomic oxygen erosion yields (the erosion yield of a material is the volume of material that is oxidized per incident oxygen atom) of materials that have been measured in low Earth orbit. It has a linear electrical

response to atomic oxygen fluence, and is capable of measuring high atomic oxygen fluences (up to $>10^{22}$ atoms/cm²), which are representative of multi-year low-Earth orbital missions (such as the International Space Station).

The durability or remaining structural lifetime of solar arrays that consist of polymer blankets on which the solar cells are attached can be predicted if one knows

the atomic oxygen fluence that the solar array blanket has been exposed to. In addition, numerous organizations that launch space experiments into low-Earth orbit want to know the accumulated atomic oxygen fluence that their materials or components have been exposed to.

The device is based on the erosion yield of pyrolytic graphite. It uses two 12° inclined wedges of graphite that are over a grit-blasted fused silica window covering a photodiode. As the wedges erode, a greater area of solar illumination reaches the photodiode. A refer-

ence photodiode is also used that receives unobstructed solar illumination and is oriented in the same direction as the pyrolytic graphite covered photodiode. The short-circuit current from the photodiodes is measured and either sent to an onboard data logger, or transmitted to a receiving station on Earth. By comparison of the short-circuit currents from the fluence-measuring photodiode and the reference photodiode, one can compute the accumulated atomic oxygen fluence arriving in the direction that the fluence monitor is pointing.

The device produces a signal that is linear with atomic oxygen fluence using a material whose atomic oxygen erosion yield has been measured over a period of several years in low-Earth orbit.

This work was done by Bruce A. Banks of the Glenn Research Center. Further information is contained in a TSP (see page 1).

Inquiries concerning rights for the commercial use of this invention should be addressed to NASA Glenn Research Center, Innovative Partnerships Office, Attn: Steven Fedor, Mail Stop 4-8, 21000 Brookpark Road, Cleveland, Ohio 44135. Refer to LEW-18639-1.



Thermal Management Tools for Propulsion System Trade Studies and Analysis

Applications include modeling and simulation in building and data center cooling analysis, and in ground-based vehicle studies.

John H. Glenn Research Center, Cleveland, Ohio

Energy-related subsystems in modern aircraft are more tightly coupled with less design margin. These subsystems include thermal management subsystems, vehicle electric power generation and distribution, aircraft engines, and flight control. Tighter coupling, lower design margins, and higher system complexity all make preliminary trade studies difficult. A suite of thermal management analysis tools has been developed to facilitate trade studies during preliminary design of air-vehicle propulsion systems.

Simulink blocksets (from MathWorks) for developing quasi-steady-state and transient system models of aircraft thermal management systems and related

energy systems have been developed. These blocksets extend the Simulink modeling environment in the thermal sciences and aircraft systems disciplines. The blocksets include blocks for modeling aircraft system heat loads, heat exchangers, pumps, reservoirs, fuel tanks, and other components at varying levels of model fidelity.

The blocksets have been applied in a first-principles, physics-based modeling and simulation architecture for rapid prototyping of aircraft thermal management and related systems. They have been applied in representative modern aircraft thermal management system studies. The modeling and simulation ar-

chitecture has also been used to conduct trade studies in a vehicle level model that incorporates coupling effects among the aircraft mission, engine cycle, fuel, and multi-phase heat-transfer materials.

This work was done by Kevin McCarthy of PC Krause & Associates and Ernie Hodge of Modelogics for Glenn Research Center. For further information contact Dr. Jeffrey Dalton, Avetec Chief Technology Officer, jdalton@avetec.org.

Inquiries concerning rights for the commercial use of this invention should be addressed to NASA Glenn Research Center, Innovative Partnerships Office, Attn: Steve Fedor, Mail Stop 4-8, 21000 Brookpark Road, Cleveland, Ohio 44135. Refer to LEW-18463-1/4-1.

Introduction to Physical Intelligence

NASA's Jet Propulsion Laboratory, Pasadena, California

A slight deviation from Newtonian dynamics can lead to new effects associated with the concept of physical intelligence. Non-Newtonian effects such as deviation from classical thermodynamic as well as quantum-like properties have been analyzed.

A self-supervised ("intelligent") particle that can escape from Brownian mo-

tion autonomously is introduced. Such a capability is due to a coupling of the particle governing equation with its own Liouville equation via an appropriate feedback. As a result, the governing equation is self-stabilized, and random oscillations are suppressed, while the Liouville equation takes the form of the Fokker-Planck equation with negative diffusion. Non-

Newtonian properties of such a dynamical system as well as thermodynamical implications have been evaluated.

This work was done by Michail Zak of Caltech for NASA's Jet Propulsion Laboratory. For more information, contact iaoffice@jpl.nasa.gov. NPO-47165

Technique for Solving Electrically Small to Large Structures for Broadband Applications

Methods are combined.

Lyndon B. Johnson Space Center, Houston, Texas

Fast iterative algorithms are often used for solving Method of Moments (MoM) systems, having a large number of unknowns, to determine current distribution and other parameters. The most commonly used fast methods in-

clude the fast multipole method (FMM), the precorrected fast Fourier transform (PFFT), and low-rank QR compression methods. These methods reduce the $O(N)$ memory and time requirements to $O(N \log N)$ by compressing the dense

MoM system so as to exploit the physics of Green's Function interactions.

FFT-based techniques for solving such problems are efficient for space-filling and uniform structures, but their performance substantially de-

grades for non-uniformly distributed structures due to the inherent need to employ a uniform global grid. FMM or QR techniques are better suited than FFT techniques; however, neither the FMM nor the QR technique can be used at all frequencies.

This method has been developed to efficiently solve for a desired parameter of a system or device that can include both electrically large FMM elements, and electrically small QR elements. The system or device is set up as an oct-tree structure that can include regions of both the FMM type and the QR type. The system is enclosed with a cube at a 0-th level, splitting the cube at the 0-th level into eight child cubes. This forms cubes at a 1-st level, recursively repeating the splitting process for cubes at successive levels until a desired number of lev-

els is created. For each cube that is thus formed, neighbor lists and interaction lists are maintained.

An iterative solver is then used to determine a first matrix vector product for any electrically large elements as well as a second matrix vector product for any electrically small elements that are included in the structure. These matrix vector products for the electrically large and small elements are combined, and a net delta for a combination of the matrix vector products is determined. The iteration continues until a net delta is obtained that is within the predefined limits. The matrix vector products that were last obtained are used to solve for the desired parameter. The solution for the desired parameter is then presented to a user in a tangible form; for example, on a display.

This work was done by Vikram Jandhyala and Indranil Chowdhury of the University of Washington for Johnson Space Center. For further information, contact the Johnson Technology Transfer Office at (281) 483-3809.

In accordance with Public Law 96-517, the contractor has elected to retain title to this invention. Inquiries concerning rights for its commercial use should be addressed to:

*Janice C. Walsh
Federal Reporting Compliance Licensing Specialist*

*UW Tech Transfer
University of Washington
4322-11th Avenue, N.E., Suite 500
Seattle, WA 98105-4608*

*E-mail: wavinvent@u.washington.edu
Refer to MSC-24439-1, volume and number of this NASA Tech Briefs issue, and the page number.*

Accelerated Adaptive MGS Phase Retrieval

NASA's Jet Propulsion Laboratory, Pasadena, California

The Modified Gerchberg-Saxton (MGS) algorithm is an image-based wavefront-sensing method that can turn any science instrument focal plane into a wavefront sensor. MGS characterizes optical systems by estimating the wavefront errors in the exit pupil using only intensity images of a star or other point source of light. This innovative implementation of MGS significantly accelerates the MGS phase retrieval algorithm by using stream-processing hardware on conventional graphics cards.

Stream processing is a relatively new, yet powerful, paradigm to allow parallel processing of certain applications that apply single instructions to multiple data (SIMD). These stream processors are designed specifically to support large-scale parallel computing on a single graphics chip. Computation-

ally intensive algorithms, such as the Fast Fourier Transform (FFT), are particularly well suited for this computing environment. This high-speed version of MGS exploits commercially available hardware to accomplish the same objective in a fraction of the original time. The exploit involves performing matrix calculations in nVidia graphic cards. The graphical processor unit (GPU) is hardware that is specialized for computationally intensive, highly parallel computation.

From the software perspective, a parallel programming model is used, called CUDA, to transparently scale multicore parallelism in hardware. This technology gives computationally intensive applications access to the processing power of the nVidia GPUs through a C/C++ programming interface. The AAMGS (Accel-

erated Adaptive MGS) software takes advantage of these advanced technologies, to accelerate the optical phase error characterization. With a single PC that contains four nVidia GTX-280 graphic cards, the new implementation can process four images simultaneously to produce a JWST (James Webb Space Telescope) wavefront measurement 60 times faster than the previous code.

This work was done by Raymond K. Lam, Catherine M. Ohara, Joseph J. Green, Siddharayappa A. Bikkannavar, Scott A. Basinger, David C. Redding, and Fang Shi of Caltech for NASA's Jet Propulsion Laboratory. For more information, contact iaoffice@jpl.nasa.gov.

The software used in this innovation is available for commercial licensing. Please contact Daniel Broderick of the California Institute of Technology at danielb@caltech.edu. Refer to NPO-47101.

Large Eddy Simulation Study for Fluid Disintegration and Mixing

This work is directly applicable to simulations of gas turbine engines and rocket engines.

NASA's Jet Propulsion Laboratory, Pasadena, California

A new modeling approach is based on the concept of large eddy simulation (LES) within which the large scales are computed and the small scales are modeled. The new approach is expected to retain the fidelity of the

physics while also being computationally efficient. Typically, only models for the small-scale fluxes of momentum, species, and enthalpy are used to reintroduce in the simulation the physics lost because the computation only re-

solves the large scales. These models are called subgrid (SGS) models because they operate at a scale smaller than the LES grid.

In a previous study of thermodynamically supercritical fluid disintegration and

mixing, additional small-scale terms, one in the momentum and one in the energy conservation equations, were identified as requiring modeling. These additional terms were due to the tight coupling between dynamics and real-gas thermodynamics. It was inferred that if these terms would not be modeled, the high density-gradient magnitude regions, experimentally identified as a characteristic feature of these flows, would not be accurately predicted without the additional term in the momentum equation; these high density-gradient magnitude regions were experimentally shown to redistribute turbulence in the flow. And it was also inferred that without the additional term in the energy equation, the heat flux magnitude could not be accurately predicted; the heat flux to the wall of combustion devices is a crucial quantity that determined necessary wall material properties.

The present work involves situations where only the term in the momentum equation is important. Without this additional term in the momentum equation, neither the SGS-flux constant-coefficient Smagorinsky model nor the SGS-flux constant-coefficient Gradient model could reproduce in LES the pressure field or the high density-gradient magnitude regions; the SGS-flux constant-coefficient Scale-Similarity model was the most successful in this endeavor although not totally satisfactory. With a model for the additional term in the momentum equation, the predictions of the constant-coefficient Smagorinsky and constant-coefficient Scale-Similarity models were improved to a certain extent; however, most of the improvement was obtained for the Gradient model. The previously derived model and a newly developed model for the addi-

tional term in the momentum equation were both tested, with the new model proving even more successful than the previous model at reproducing the high density-gradient magnitude regions. Several dynamic SGS-flux models, in which the SGS-flux model coefficient is computed as part of the simulation, were tested in conjunction with the new model for this additional term in the momentum equation. The most successful dynamic model was a “mixed” model combining the Smagorinsky and Gradient models.

This work is directly applicable to simulations of gas turbine engines (aeronautics) and rocket engines (astronautics).

This work was done by Josette Bellan and Ezgi Taskınoğlu of Caltech for NASA’s Jet Propulsion Laboratory. For more information, contact iaoffice@jpl.nasa.gov. NPO-47040

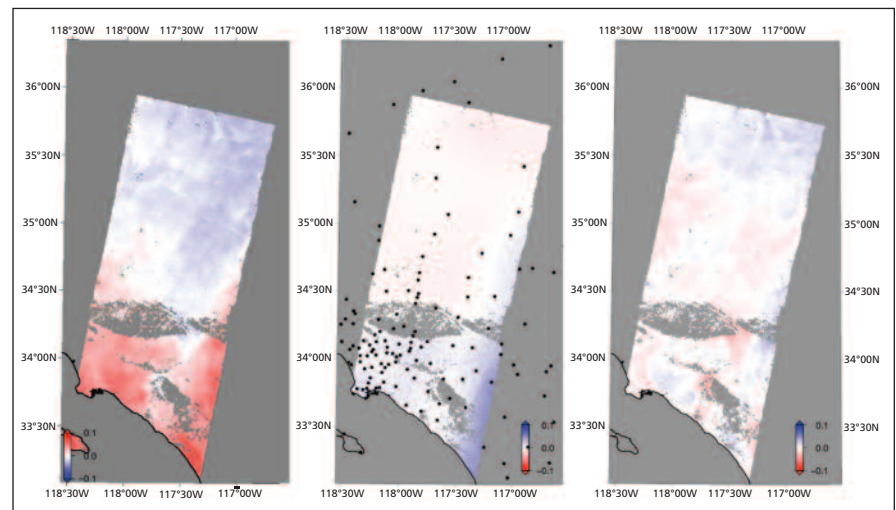
➤ Tropospheric Correction for InSAR Using Interpolated ECMWF Data and GPS Zenith Total Delay

This technique could be used in environmental remote sensing applications.

NASA’s Jet Propulsion Laboratory, Pasadena, California

To mitigate atmospheric errors caused by the troposphere, which is a limiting error source for spaceborne interferometric synthetic aperture radar (InSAR) imaging, a tropospheric correction method has been developed using data from the European Centre for Medium-Range Weather Forecasts (ECMWF) and the Global Positioning System (GPS).

The ECMWF data was interpolated using a Stretched Boundary Layer Model (SBLM), and ground-based GPS estimates of the tropospheric delay from the Southern California Integrated GPS Network were interpolated using modified Gaussian and inverse distance weighted interpolations. The resulting Zenith Total Delay (ZTD) correction maps have been evaluated, both separately and using a combination of the two data sets, for three short-interval InSAR pairs from Envisat during 2006 on an area stretching from northeast from the Los Angeles basin towards Death Valley. Results show that the root mean square (rms) in the InSAR images was greatly reduced, meaning a significant reduction in the atmospheric noise of up to 32 percent. However, for some of the images, the rms increased and large errors remained after apply-



The Original InSAR Image (left), the GPS ZTD Difference Correction Map (center), and the corrected InSAR Image (right). The black dots in the middle image correspond to the locations of the GPS stations.

ing the tropospheric correction. The residuals showed a constant gradient over the area, suggesting that a remaining orbit error from Envisat was present. The orbit reprocessing in ROI_pac and the plane fitting both require that the only remaining error in the InSAR image be the orbit error. If this is not fulfilled, the correction can be made

anyway, but it will be done using all remaining errors assuming them to be orbit errors. By correcting for tropospheric noise, the biggest error source is removed, and the orbit error becomes apparent and can be corrected for.

After reprocessing the InSAR images using re-estimated satellite orbits, the overall rms reduction (using both tro-

ospheric and orbit correction) spanned from 15 to 68 percent. With this tropospheric correction, low-frequency errors can be removed from InSAR images. Additionally, results show that for days with high-quality ECMWF data, the SBLM ZTD correction performs as well as the GPS ZTD correction. Finally, the tropospheric correction enabled

orbit correction, and by correcting for both errors, the quality of the InSAR images increased significantly.

By correcting for the troposphere, other errors become visible. The main contributor to the remaining errors is uncertainties with determining the satellite orbit. Because the orbit error is now separated from the tropospheric error, the

orbit can be corrected for more accurately.

This work was done by Frank H. Webb, Evan F. Fishbein, Angelyn W. Moore, Susan E. Owen, Eric J. Fielding, and Stephanie L. Granger of Caltech and Fredrik Björndahl and Johan Löfgren of Chalmers University of Technology for NASA's Jet Propulsion Laboratory. Further information is contained in a TSP (see page 1). NPO-46918

➤ Technique for Calculating Solution Derivatives With Respect to Geometry Parameters in a CFD Code

John H. Glenn Research Center, Cleveland, Ohio

A solution has been developed to the challenges of computation of derivatives with respect to geometry, which is not straightforward because these are not typically direct inputs to the computational fluid dynamics (CFD) solver. To overcome these issues, a procedure has been devised that can be used without having access to the mesh generator, while still being applicable to all types of meshes. The basic approach is inspired by the mesh motion algorithms used to deform the interior mesh nodes in a smooth manner when the surface nodes, for example, are in a fluid structure interaction problem. The general idea is to model the mesh edges and nodes as constituting a spring-mass system. Changes to boundary node locations are propa-

gated to interior nodes by allowing them to assume their new equilibrium positions, for instance, one where the forces on each node are in balance.

The main advantage of the technique is that it is independent of the volumetric mesh generator, and can be applied to structured, unstructured, single- and multi-block meshes. It essentially reduces the problem down to defining the surface mesh node derivatives with respect to the geometry parameters of interest. For analytical geometries, this is quite straightforward. In the more general case, one would need to be able to interrogate the underlying parametric CAD (computer aided design) model and to evaluate the derivatives either analytically, or by a finite difference tech-

nique. Because the technique is based on a partial differential equation (PDE), it is applicable not only to forward mode problems (where derivatives of all the output quantities are computed with respect to a single input), but it could also be extended to the adjoint problem, either by using an analytical adjoint of the PDE or a discrete analog.

This work was done by Sanjay Mathur of Jabiru Software and Services, LLC, for Glenn Research Center. Further information is contained in a TSP (see page 1)

Inquiries concerning rights for the commercial use of this invention should be addressed to NASA Glenn Research Center, Innovative Partnerships Office, Attn: Steve Fedor, Mail Stop 4-8, 21000 Brookpark Road, Cleveland, Ohio 44135. Refer to LEW-18499-1.

➤ Acute Radiation Risk and BRYNTRN Organ Dose Projection Graphical User Interface

This program estimates the whole-body effective dose, organ doses, and acute radiation sickness symptoms.

Lyndon B. Johnson Space Center, Houston, Texas

The integration of human space applications risk projection models of organ dose and acute radiation risk has been a key problem. NASA has developed an organ dose projection model using the BRYNTRN with SUM DOSE computer codes, and a probabilistic model of Acute Radiation Risk (ARR). The codes BRYNTRN and SUM DOSE are a Baryon transport code and an output data processing code, respectively. The risk projection models of organ doses and ARR take the output from BRYNTRN as an input to their calculations. With a graphical user interface

(GUI) to handle input and output for BRYNTRN, the response models can be connected easily and correctly to BRYNTRN. A GUI for the ARR and BRYNTRN Organ Dose (ARRBOD) projection code provides seamless integration of input and output manipulations, which are required for operations of the ARRBOD modules.

The ARRBOD GUI is intended for mission planners, radiation shield designers, space operations in the mission operations directorate (MOD), and space biophysics researchers. BRYNTRN code operation requires extensive

input preparation. Only a graphical user interface (GUI) can handle input and output for BRYNTRN to the response models easily and correctly. The purpose of the GUI development for ARRBOD is to provide seamless integration of input and output manipulations for the operations of projection modules (BRYNTRN, SLMDOSE, and the ARR probabilistic response model) in assessing the acute risk and the organ doses of significant Solar Particle Events (SPEs).

The assessment of astronauts' radiation risk from SPE is in support of mis-

sion design and operational planning to manage radiation risks in future space missions. The ARRBOD GUI can identify the proper shielding solutions using the gender-specific organ dose assessments in order to avoid ARR symptoms, and to stay within the current NASA short-term dose limits. The quantified evaluation of ARR severities based on any given shielding configuration and a

specified EVA or other mission scenario can be made to guide alternative solutions for attaining determined objectives set by mission planners.

The ARRBOD GUI estimates the whole-body effective dose, organ doses, and acute radiation sickness symptoms for astronauts, by which operational strategies and capabilities can be made for the protection of astronauts from

SPEs in the planning of future lunar surface scenarios, exploration of near-Earth objects, and missions to Mars.

This work was done by Francis A. Cucinotta of Johnson Space Center, and Shaowen Hu, Hateni N. Nounu, and Myung-Hee Y. Kim of the Universities Space Research Association. Further information is contained in a TSP (see page 1). MSC-24789-1

➤ Probabilistic Path Planning of Montgolfier Balloons in Strong, Uncertain Wind Fields

This algorithm can be used for underwater unmanned vehicles for automated scientific data collection and for military uses.

NASA's Jet Propulsion Laboratory, Pasadena, California

Lighter-than-air vehicles such as hot-air balloons have been proposed for exploring Saturn's moon Titan, as well as other bodies with significant atmospheres. For these vehicles to navigate effectively, it is critical to incorporate the effects of surrounding wind fields, especially as these winds will likely be strong relative to the control authority of the vehicle. Predictive models of these wind fields are available, and previous research has considered problems of planning paths subject to these predicted forces. However, such previous work has considered the wind fields as known *a priori*, whereas in practical applications, the actual wind vector field is not known exactly and may deviate significantly from the wind velocities estimated by the model.

A probabilistic 3D path-planning algorithm was developed for balloons to use uncertain wind models to generate time-efficient paths. The nominal goal of the algorithm is to determine what altitude and what horizontal actuation, if any is available on the vehicle, to use to reach a

particular goal location in the least expected time, utilizing advantageous winds. The solution also enables one to quickly evaluate the expected time-to-goal from any other location and to avoid regions of large uncertainty. This method is designed for balloons in wind fields but may be generalized for any buoyant vehicle operating in a vector field.

To prepare the planning problem, the uncertainty in the wind field is modeled. Then, the problem of reaching a particular goal location is formulated as a Markov decision process (MDP) using a discretized space approach. Solving the MDP provides a policy of what actuation option (how much buoyancy change and, if applicable, horizontal actuation) should be selected at any given location to minimize the expected time-to-goal. The results provide expected time-to-goal values from any given location on the globe in addition to the action policy.

This stochastic approach can also provide insights not accessible by deterministic methods; for example, one can evaluate variability and risk associated with

different scenarios, rather than only viewing the expected outcome.

The resulting path-planning tool is a general-purpose guidance algorithm that can be applied to exploration balloons on any moon/planet with atmosphere, including Titan, Mars, Venus, and gas giants, provided the wind field models are available. The algorithm is particularly useful for mission planning and trade studies because it not only delivers the optimal expected path, but also provides insights into the variability and risk associated with different mission scenarios (e.g., under different wind variability or vehicle capabilities). Finally, these techniques may be useful for other variably buoyant vehicles operating in strong vector fields, such as underwater vehicles in ocean currents, which may have additional scientific or military significance.

This work was done by Michael Wolf, James C. Blackmore, and Yoshiaki Kuwata of Caltech for NASA's Jet Propulsion Laboratory. For more information, contact iaoffice@jpl.nasa.gov. NPO-47111



Books & Reports

Flight Simulation of ARES in the Mars Environment

A report discusses using the Aerial Regional-scale Environmental Survey (ARES) light airplane as an observation platform on Mars in order to gather data. It would have to survive insertion into the atmosphere, fly long enough to meet science objectives, and provide a stable platform.

The feasibility of such a platform was tested using the Langley Standard Real-Time Simulation in C++. The unique features of LaSRS++ are: full, six-degrees-of-freedom flight simulation that can be used to evaluate the performance of the aircraft in the Martian environment; capability of flight analysis from start to finish; support of Monte Carlo analysis of aircraft performance; and accepting initial conditions from POST results for the entry and deployment of the entry body.

Starting with a general aviation model, the design was tweaked to maintain a stable aircraft under expected Martian conditions. Outer mold lines were adjusted based on experience with the Martian atmosphere. Flight control was modified from a vertical acceleration control law to an angle-of-attack control law. Navigation was modified from a vertical acceleration control system to an alpha control system. In general, a pattern of starting with simple models with well-understood behaviors was selected and modified during testing.

This work was done by P. Sean Kenney and Mark A. Croom of Langley Research Center. Further information is contained in a TSP (see page 1). LAR-17458

Low-Outgassing Photogrammetry Targets for Use in Outer Space

A short document discusses an investigation of materials for photogrammetry targets for highly sensitive optical scientific instruments to be operated in outer space and in an outer-space-environment-simulating thermal vacuum chamber on Earth. A key consideration in the selection of photogrammetry-target materials for vacuum environments is the need to prevent contamination that could degrade the optical responses of the instruments. Therefore, in addition

to the high levels and uniformity of reflectivity required of photogrammetry-target materials suitable for use in air, the materials sought must exhibit minimal outgassing.

Commercially available photogrammetry targets were found to outgas excessively under the thermal and vacuum conditions of interest; this finding prompted the investigators to consider optically equivalent or superior, lower-outgassing alternative target materials. The document lists several materials found to satisfy the requirements, but does not state explicitly whether the materials can be used individually or must be combined in the proper sequence into layered target structures. The materials in question are an aluminized polyimide tape, an acrylic pressure-sensitive adhesive, a 500-Å-thick layer of vapor-deposited aluminum, and spherical barium titanate glass beads having various diameters from 20 to 63 μm .

This work was done by Jason N. Gross, Henry Sampler, and Benjamin B. Reed of Goddard Space Flight Center. Further information is contained in a TSP (see page 1). GSC-15373-1

Planning the FUSE Mission Using the SOVA Algorithm

Three documents discuss the Sustainable Objective Valuation and Attainability (SOVA) algorithm and software as used to plan tasks (principally, scientific observations and associated maneuvers) for the Far Ultraviolet Spectroscopic Explorer (FUSE) satellite. SOVA is a means of managing risk in a complex system, based on a concept of computing the expected return value of a candidate ordered set of tasks as a product of pre-assigned task values and assessments of attainability made against qualitatively defined strategic objectives.

For the FUSE mission, SOVA autonomously assembles a week-long schedule of target observations and associated maneuvers so as to maximize the expected scientific return value while keeping the satellite stable, managing the angular momentum of spacecraft attitude-control reaction wheels, and striving for other strategic objectives. A six-degree-of-freedom model of the spacecraft is used in simulating the tasks, and the attainability of a task is calcu-

lated at each step by use of strategic objectives as defined by use of fuzzy inference systems. SOVA utilizes a variant of a graph-search algorithm known as the A* search algorithm to assemble the tasks into a week-long target schedule, using the expected scientific return value to guide the search.

This work was done by Jim Lanzi, Scott Heatwole, and Philip R. Ward of Goddard Space Flight Center and Thomas Civeit, Humberto Calwani, Jeffrey W. Kruk, and Anatoly Suchkov of Johns Hopkins University. Further information is contained in a TSP (see page 1). GSC-15436-1

Monitoring Spacecraft Telemetry Via Optical or RF Link

A patent disclosure document discusses a photonic method for connecting a spacecraft with a launch vehicle upper-stage telemetry system as a means for monitoring a spacecraft's health and status during and right after separation and deployment. This method also provides an efficient opto-coupled capability for prelaunch built-in-test (BIT) on the ground to enable more efficient and timely integration, preflight checkout, and a means to obviate any local EMI (electromagnetic interference) during integration and test. Additional utility can be envisioned for BIT on other platforms, such as the International Space Station (ISS).

The photonic telemetry system implements an optical free-space link with a divergent laser transmitter beam spoiled over a significant cone angle to accommodate changes in spacecraft position without having to angle track it during deployment. Since the spacecraft may lose attitude control and tumble during deployment, the transmitted laser beam interrogates any one of several low-profile meso-scale retro-reflective spatial light modulators (SLMs) deployed over the surface of the spacecraft. The return signal beam, modulated by the SLMs, contains health, status, and attitude information received back at the launch vehicle. Very compact low-power opto-coupler technology already exists for the received signal (requiring relatively low bandwidths, e.g., ≤ 200 kbps) to enable transfer to a forward pass RF relay from the launch vehicle to TDRSS

(Tracking and Data Relay Satellite System) or another recipient. The link would be active during separation and post-separation to monitor spacecraft health, status, attitude, or other data inventories until attitude recovery and ground control can be re-established. An optical link would not interfere with the existing upper stage telemetry and beacon systems, thus meeting launch vehicle EMI environmental constraints.

This work was done by K.B. Fielhauer and B.G. Boone for Goddard Space Flight Center. Further information is contained in a TSP (see page 1). GSC-14832-1

Robust Thermal Control of Propulsion Lines for Space Missions

A document discusses an approach to insulating propulsion lines for spacecraft. In spacecraft that have propulsion lines that are located externally

with open bus architecture, the lines are typically insulated by Multi Layer Insulation (MLI) blankets. MLI on propulsion lines tends to have large and somewhat random variances in its heat loss properties (effective emittance) from one location to the next, which makes it an un-robust approach to control propulsion line temperatures. The approach described here consists of a “clamshell” design in which the inner surface of the shell is coated with low-emissivity aluminized Kapton tape, and the outer surface is covered with black tape. This clamshell completely encloses the propulsion line. The line itself is covered with its heater, which in turn, is covered completely with black tape.

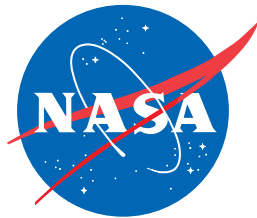
This approach would be low in heater power needs because even though the outer surface of the prop line (and its heater) is covered with black tape as well as the outer surface of the clamshell, the

inner surface of the clamshell is covered with low-emissivity aluminized Kapton tape. Hence, the heat loss from the line will be small and comparable to the MLI based one.

In terms of contamination changing the radiative properties of surfaces, since the clamshell’s inner surface is always protected during handling and is only installed after all the work on the prop line has been completed, the controlling surface, which is the clamshell’s inner surface, is always in pristine condition.

This proposed design allows for a much more deterministic and predictable design using a very simple and implementable approach for thermal control. It also uses low heater power and is robust to handling and contamination during and after implementation.

This work was done by Pradeep Bhandari of Caltech for NASA’s Jet Propulsion Laboratory. Further information is contained in a TSP (see page 1). NPO-47441



National Aeronautics and
Space Administration